

VeriLLM: A Lightweight Framework for Publicly Verifiable Decentralized Inference

Ke Wang

Gradient Network

Email: wangke@gradient.network

Bill Shi

Gradient Network

Email: tianyu.shi@gradient.network

Lynn Ai

Gradient Network

Email: lynn@gradient.network

Zishuo Zhao

Gradient Network

Email: zishuo2@illinois.edu

Libin Xia

Peking University

Email: lbxia@stu.pku.edu.cn

Felix Qu

National University of Singapore

Email: 2382036672@qq.com

Xinyuan Song

Gradient Network

Email: xinyuan.song@emory.edu

Chris Tong

Gradient Network

Email: ChrisT@gradient.network

Eric Yang

Gradient Network

Email: eric@gradient.network

Abstract—Decentralized inference provides a scalable and resilient paradigm for serving large language models (LLMs), enabling distributed resource utilization and reducing reliance on centralized providers. However, in a permissionless environment without trusted nodes, ensuring the correctness of model outputs remains a core challenge. We introduce VeriLLM, a publicly verifiable protocol for decentralized LLM inference that achieves security under a one-honest-verifier assumption while maintaining practical efficiency. VeriLLM combines lightweight empirical rerunning with cryptographic commitments, allowing verifiers to validate results at approximately 1% of the underlying inference cost. To prevent verification bottlenecks, we design an isomorphic inference–verification architecture that multiplexes both inference and verification roles across the same GPU workers. This design (i) improves GPU utilization and overall throughput, (ii) enlarges the effective validator set, enhancing robustness and liveness, and (iii) enforces task indistinguishability to prevent node-specific optimizations or selective behavior. Through theoretical analysis and system-level evaluation, we show that VeriLLM achieves reliable public verifiability with minimal overhead, offering a practical foundation for trustworthy and scalable decentralized LLM inference.

1. Introduction

The recent surge of Large Language Models (LLMs) is driven by their broad utility in diverse domains, including software development [1] and creative content generation, resulting in widespread adoption across both industrial and academic settings [2], [3], [4]. However, this progress exposes a fundamental weakness in current AI infrastructure: the computational and model resources required to support large-scale inference are heavily centralized within a few dominant technology providers [5], [6], [7]. Such concentration leads to systemic risks, including privacy violations,

restricted access, single points of failure, and monopolistic control over core AI capabilities [5], [8], [9], [10].

To mitigate these risks, *decentralized inference* [11], [12], [13], [14], [15], [16], [17], [18] has emerged as a promising direction. By distributing computation across independent providers, decentralized systems aim to achieve openness, fault tolerance, and fairer access to AI resources [19], [20], [21], [22]. This paradigm enables verifiable collaboration among untrusted nodes and democratizes access to model execution, thereby improving transparency and resilience of large-scale AI deployments [6], [20], [23], [24].

A central challenge in decentralized inference, however, is **verifiable correctness**. In a permissionless network, inference providers may be faulty, compromised, or economically motivated to skip computation. Without a mechanism to verify results, participants cannot ensure the integrity of model outputs [25], [26], [27], [28], [29]. This issue extends beyond adversarial behavior: providers often apply hidden optimizations—such as reduced numerical precision, pruned or distilled models, modified prompts, or compressed key-value caches—that degrade output fidelity [30], [31], [32], [33], [34], [35]. As a result, independent verification becomes an operational necessity for any decentralized inference infrastructure [36].

Existing approaches to verification face critical efficiency and deployability limitations. Cryptographic proof systems, including zero-knowledge proofs (ZKPs), can formally attest to correctness but remain computationally prohibitive: current frameworks introduce overheads several orders of magnitude larger than native inference, particularly for transformer-scale models [37], [38], [39], [40]. Consensus-based schemes, in contrast, rely on redundant replication and majority voting or interactive verification games. These methods require strong synchrony or honest-majority assumptions and suffer from high latency and resource overhead [41], [42], [43]. Furthermore, both proof-

based and replication-based approaches align poorly with modern blockchain environments, where on-chain verification of large ML proofs is expensive and deterministic numerical reproducibility across heterogeneous hardware remains unsolved.

To address these limitations, we introduce **VeriLLM**, a publicly verifiable protocol for decentralized LLM inference designed for efficiency, security, and scalability. VeriLLM achieves verifiability under a *one-honest-verifier* assumption, enabling robust correctness guarantees without relying on honest-majority trust. The system combines lightweight empirical rerunning with cryptographic commitments, reducing the average verification overhead to about 1% of standard inference cost. In addition, a peer-auditing mechanism ensures collusion resistance and discourages lazy verification, enabling open, reliable, and low-cost validation of large-scale model execution.

To achieve security under the one-honest-verifier assumption while maintaining low verification cost, we design a hybrid architecture that integrates empirical rerunning with cryptographic verification. The proposed system consists of three core components that collectively ensure both efficiency and verifiability.

(1) Commitment of Intermediate States. During computation, all intermediate hidden states are committed to Merkle trees [44], with their root hashes recorded on-chain. These commitments yield tamper-evident logs, serving as binding evidence for subsequent verification and dispute resolution.

(2) Randomized Empirical Verification. A verifiable random function (VRF) [45] determines unpredictable verification indices. At these positions, any verifier can re-execute the corresponding computations off-chain and compare the locally obtained results with the committed Merkle values. This sampling-based mechanism substantially reduces verification overhead while maintaining probabilistic soundness.

(3) Dispute-Resolution Protocol. In the event of inconsistencies, any honest verifier may initiate a dispute-resolution procedure by submitting Merkle proofs that demonstrate mismatches between recomputed and committed states. When empirical verification is insufficient for resolution, the protocol escalates to zero-knowledge proofs [46], [47] to provide conclusive adjudication.

Through this hybrid framework, our system ensures that even a single honest verifier can detect and prove computational misconduct with overwhelming probability, while keeping the expected verification cost low.

Building on this foundation, we further optimize the verification path by exploiting the inherent computational structure of large language model (LLM) inference. A standard inference pipeline consists of a *Prefill* phase followed by an autoregressive *Decoder* phase, with the latter dominating total runtime [48]. We observe that when the complete output sequence is available to verifiers, the expensive Decoder phase need not be re-executed. Instead, verifiers can perform only the Prefill computation to validate correctness, as the subsequent token generation is a deterministic function of

Prefill activations. This selective recomputation significantly reduces the verification overhead—approximately 1% of full inference cost—without compromising fidelity or verifiability.

Low verification cost alone is not sufficient in a permissionless network: validation must also be publicly auditable and resistant to non-participation. To achieve public verifiability and prevent lazy verification, VeriLLM augments the above optimization with a blockchain-assisted protocol that provides transparent coordination and accountable reporting, while preserving low on-chain cost. Intensive checks are executed off-chain by selected verifiers, and the blockchain performs lightweight consistency tests and resolves disputes. Sampling randomness is derived from on-chain verifiable random functions (VRFs) [45], which select unpredictable hidden-state positions for audit. For each sample, verifiers submit Merkle openings [44] with minimal recomputation to attest that the required steps were executed. A peer-consistency mechanism then compares submissions and rewards alignment with the distribution expected from honest computation, which discourages collusion and maintains liveness without heavy replication.

Building on this foundation, we replace the conventional heterogeneous Inferencer–Verifier separation with an **isomorphic inference–verification network** in which all GPU workers multiplex both roles. The scheduler randomly assigns inference and verification jobs across the same hardware pool, and each worker executes both types without explicit role awareness. This task indistinguishability prevents behavior conditioned on job type, mitigates selective optimization, and improves hardware utilization by amortizing verification across the same computational substrate. As a result, the architecture simultaneously increases throughput and expands the effective validator set, strengthening robustness and decentralization.

Finally, VeriLLM undergoes comprehensive robustness evaluation against realistic threats such as quantized computation, early termination, and forged-output replay. The combination of Merkle commitments, VRF-based sampling, and on-chain dispute resolution ensures that any single honest verifier can detect and prove inconsistency with overwhelming probability. This establishes practical correctness guarantees without relying on replication or majority consensus.

1.1. Summary of Contributions

- **Single-Honest-Verifier Security:** VeriLLM achieves correctness guarantees under a one-honest-verifier assumption through Merkle commitments, VRF-based sampling, and on-chain dispute resolution.
- **Minimal Verification Cost:** By exploiting the structural separation of Prefill and Decoder phases in transformer inference, VeriLLM reduces verification overhead to approximately 1% of full inference cost.
- **Public and Collusion-Resistant Verification:** A blockchain-based two-layer verification mechanism and peer-consistency incentives ensure that all verifiers

perform computations honestly while keeping on-chain operations lightweight.

- **Isomorphic Inference–Verification Network:** The architecture multiplexes inference and verification roles across identical GPU workers, improving throughput and preventing task-specific adversarial behavior.
- **Comprehensive Security Evaluation:** We demonstrate robustness against practical attack vectors and show that VeriLLM provides scalable, low-cost, and publicly verifiable decentralized inference.

2. Design Goals and Threat Alignment

This section formalizes the security and system design goals of **VeriLLM** and establishes their alignment with the assumed adversarial capabilities. Our design aims to provide verifiable, tamper-evident, and publicly auditable large language model (LLM) inference in a decentralized environment without relying on trusted majorities or centralized coordination [19], [26], [27].

2.1. Adversarial Capabilities

We consider a permissionless network composed of three types of participants: *Inferencers*, *Verifiers*, and a *Scheduler*. Each participant may deviate from the prescribed protocol to gain computational or economic advantage [25], [41].

- **C1: Malicious Inferencer.** An Inferencer may attempt to reduce computation cost by (i) running a smaller or quantized model, (ii) terminating early, or (iii) reusing cached or fabricated hidden states while pretending to produce valid outputs [37], [38].
- **C2: Lazy or Colluding Verifiers.** A Verifier may skip recomputation and submit a verdict opportunistically, or collude with other verifiers or the Inferencer to falsely validate an incorrect computation [29], [40].
- **C3: Byzantine Scheduler.** The Scheduler may selectively relay, alter, or censor messages; it may attempt to bias role assignment or falsify commitments to conceal misbehavior [30].
- **C4: Observation and Timing Adversary.** The adversary can observe network-level messages and timing patterns in an attempt to infer whether a node is serving inference or verification, and may adapt behavior based on such information [49].
- **C5: On-chain Adversary.** Attackers may attempt to bias or replay randomness, forge signatures, or submit inconsistent commitments to gain advantage in the commit–reveal process [45], [50].

Smart contracts are assumed to execute correctly as specified. Cryptographic primitives (hashes, digital signatures, and VRFs) are assumed secure under standard assumptions (collision resistance, EUF-CMA, unpredictability).

2.2. Design Goals

VeriLLM is designed to achieve the following system and security goals in the presence of adversaries with capabilities C1–C5.

G1. Public Verifiability. *Any participant can verify inference correctness without relying on trust or replication.* All hidden states and token outputs are bound by cryptographic commitments and, through a commit–then–sample procedure [39], any participant can open selected entries and check them against the model specification. This goal directly mitigates C1 and C2 by allowing verifiable detection of computation deviation or lazy verification. The verification process is auditable both off-chain (via hidden-state recomputation) and on-chain (via sampled scalar checks).

G2. Low Overhead. *Verification overhead remains below 1% of the total inference cost.* The scheme achieves this by limiting on-chain operations to sampled scalar openings rather than full tensor uploads, and by parallelizing verifier recomputation across layer segments [51]. This goal ensures practical deployability under realistic hardware and network conditions, addressing the performance constraints implied by C1 (economic motivation to cheat).

G3. One-Honest-Verifier Security. *Correctness is guaranteed as long as at least one verifier executes the protocol honestly.* Even if all but one verifier collude with the Inferencer or Scheduler, the presence of a single honest verifier ensures that inconsistencies or forged hidden states will be revealed either through the on-chain sampling phase or via zero-knowledge dispute proofs [38], [40]. This property directly counters C2 and C3 by removing the need for a majority or trusted quorum.

G4. Deterministic Accountability. *Every message and hidden-state relay is traceable to a verifiable, signed commitment.* Each segment boundary state is committed via a Merkle root [44] and signed by the responsible node. These signatures are registered on-chain, ensuring that any alteration, omission, or forgery by a malicious Scheduler (C3) or Inferencer (C1) is cryptographically detectable. This binding of state to identity guarantees tamper-evident trace integrity.

G5. Task-Type Indistinguishability. *Workers cannot distinguish whether a job is an inference or a verification task.* Inferencers and Verifiers receive identical message formats and API calls from the Scheduler, preventing selective deviation based on task type (mitigating C4). A node that attempts to skip verification will be caught with high probability during unpredictable on-chain sampling [11].

G6. Compatibility with Decentralized Deployment. *The protocol operates robustly across heterogeneous GPUs and compute environments.* VeriLLM tolerates bounded floating-point divergence by using calibrated statistical thresholds in hidden-state comparison [52]. This ensures that cross-device verification remains feasible and fair while preventing adversaries from exploiting hardware-level drift to mask malicious changes.

2.3. Threat–Goal Alignment

Table 1 summarizes the alignment between adversarial capabilities and the corresponding design goals that mitigate each threat.

TABLE 1. THREAT–GOAL ALIGNMENT MATRIX FOR VERILLM.

Adversarial Capability	G1	G2	G3	G4	G5	G6
C1. Malicious Inference	✓		✓	✓		✓
C2. Lazy/Colluding Verifier	✓		✓		✓	
C3. Byzantine Scheduler			✓	✓		
C4. Observation/Timing Adversary					✓	
C5. On-chain Adversary	✓			✓		

The combination of these goals forms a security envelope suited for large-scale decentralized inference. Public verifiability (G1) and deterministic accountability (G4) guarantee that every computation step is externally auditable. Low-overhead design (G2) ensures practical adoption without compromising latency or throughput. The one-honest-verifier guarantee (G3) provides strong correctness in adversarial environments, while task-type indistinguishability (G5) closes adaptive attack channels. Finally, cross-device compatibility (G6) grounds the protocol in realistic heterogeneous hardware deployments [51], [52]. Together, these principles ensure that VeriLLM achieves transparent, efficient, and verifiable LLM inference under adversarial conditions typical of open, decentralized systems.

3. Related Work

3.1. Activation Sampling & Compact Commitment

Lightweight methods verify inference integrity by selectively committing to critical activation states. TOPLOC/INTELLECT [33] commits to the top-128 final-layer activations every 32 tokens, compressing data 1000 \times via polynomial congruence (258 bytes per commitment). However, its verification process requires a trusted third party to re-run the computation and provide a ground truth, which reintroduces a central trust assumption. TensorBlock [53] extends this to KV-cache sampling using deterministic token/layer selection, enabling validators to recompute partial trajectories from checkpoints. VeriSplit [54] supports private outsourcing through linear operator masking: clients add noise to inputs, workers return encrypted activations, and clients locally denoise results using precomputed terms, with Merkle trees enabling partial verification. However, their probabilistic security cannot guarantee the detection of sophisticated model tampering, and input privacy relies on noise injection techniques that are vulnerable to advanced reconstruction attacks.

3.2. Zero-Knowledge Machine Learning (ZKML)

Sumcheck-based Protocols: zkCNN [55] accelerates convolution verification by transforming operations to the

frequency domain. zkLLM [39] reduces communication by 90% for non-arithmetic operations (e.g., Softmax) via the tlookup protocol and exploits translation invariance. QAP-based Protocols: vCNN [56] represents convolutions as Quadratic Polynomial Programs (QPP), reducing multiplicative gates exponentially. pvCNN [57] further optimizes tensor operations via Quadratic Matrix Programs (QMP) and batch verification. ZKML [38] offers modular circuit design with 43 pre-built layer circuits and automated optimization. zkGPT [40] leverages multi-thread parallelization for LLM inference-proof acceleration. Lookup arguments [58] enable matrix-level privacy with 30% faster proofs. VOLE-based Protocols: Mystique [59] achieves sublinear communication for matrix multiplication using sVOLE-based tensor compression. Recent frameworks [60] optimize nonlinear functions via table lookups and digital decomposition, reducing constraints by over 99%.

System & Hardware Optimization: zkLoRA [61] supports verifiable fine-tuning via incremental proofs for LoRA modules. EZKL [37] automates ZKP circuit generation from ONNX models. DeepProve [62] accelerates GPU-based ZKML (54–158 \times faster proofs via parallelized SNARKs). Sertn [63] employs optimistic “Staked Deferred Proofs” with economic slashing for invalid results. However, these methods impose prohibitive prover costs (hours per inference), require trusted setups, and suffer from rigidity in supporting novel architectures due to circuit specialization.

However, these works come with severe drawbacks, including prohibitive prover costs (often hours per inference), the need for trusted setups in many schemes, and architectural rigidity that hinders support for novel operators due to specialized circuit designs.

3.3. Trusted Execution Environments (TEEs)

Atoma Network [64] combines TEE attestation with sampling-based consensus for deterministic execution. evML [65] uses TEE-based remote attestation (e.g., Google/Apple frameworks) with probabilistic auditing. nesa.ai [66] orchestrates heterogeneous TEEs for secure multi-party inference. Phala Network [67] extends this paradigm by providing a “Confidential AI” cloud platform that enables standard Dockerized AI applications to run within GPU-equipped TEEs. However, they inherit vulnerabilities to side-channel exploits (e.g., cache-timing attacks), centralize trust in proprietary hardware (Intel SGX/ARM TrustZone), and exhibit limited auditability across heterogeneous environments.

3.4. Consensus & Optimistic Approaches

Verde [41] employs optimistic dispute resolution, recomputing only divergent operators (e.g., single attention heads) to minimize overhead. Mira [42] leverages multi-model consensus against hallucinations using domain-specific thresholds. Ambient [43] introduces Proof-of-Logits (PoL), hashing intermediate logits for spot-check verification at < 0.1% overhead. However, they introduce delayed finality during

dispute windows and implicitly assume honest majority participation.

4. Background & Problem Statements

Full-Sequence Prefill for Parallel Verification. Autoregressive large language models (LLMs) rely on causal (left-to-right) self-attention, in which each hidden state h_t depends on all preceding tokens $\{x_1, \dots, x_{t-1}\}$. This dependency constrains the Decoder to operate sequentially, forming the dominant computational bottleneck in inference. Practical serving systems mitigate this through a *Prefill* phase that computes the contextual representations for all prompt tokens in parallel and materializes the key-value (KV) cache, allowing subsequent token-by-token decoding to reuse these cached features [48], [51], [68]. At verification time, this architectural separation becomes even more advantageous: since the verifier observes the full input–output sequence (x_1, \dots, x_T) , it can execute a single forward pass under the causal mask to recover all hidden states simultaneously, without performing the autoregressive loop.

Formally, let \mathcal{F}_θ denote the LLM parameterized by θ , and $H = \mathcal{F}_\theta(X)$ represent the sequence of hidden activations for token matrix $X \in \mathbb{R}^{T \times d_{\text{model}}}$ under causal masking. Given the full sequence, the verifier computes:

$$H' = \mathcal{F}_\theta(X_{\text{prompt}} \| X_{\text{output}}), \quad (1)$$

where $\|$ denotes concatenation. Since H' deterministically reconstructs all token representations, it serves as a sufficient statistic for verifying computational consistency. Let C_{verify} and C_{infer} denote the respective computational costs of verification and inference. Empirically, the ratio satisfies

$$\frac{C_{\text{verify}}}{C_{\text{infer}}} = \frac{T_{\text{prompt}}}{T_{\text{prompt}} + T_{\text{output}}} = 0.01, \quad (2)$$

indicating that verification requires only about 1% of total inference compute. This structural reuse renders verification nearly cost-free while preserving full fidelity of hidden-state comparison.

Lazy Verification. A naive verification baseline re-executes the entire model forward pass under identical hyperparameters and compares the resulting hidden states with those reported by the Inferencer. However, because honest inference is the common case, verifiers have an incentive to skip computation and submit a trivial `True` verdict—an instance of the *lazy-verification problem*. Such behavior gradually undermines system integrity and leads to unverifiable results.

To address this, VeriLLM employs a lightweight *commit–sample–check* protocol. Each verifier v_i commits to its hidden states by posting a Merkle root $r_i = \text{Merkle}(H_i)$ [44]. After commitments are finalized, a smart contract derives random challenge indices $\mathcal{S} = \{s_1, \dots, s_k\}$ from a verifiable random function (VRF) [45], ensuring unpredictability and fairness. Each verifier must open the corresponding leaves $\{H_i[s_j]\}_{j=1}^k$ and submit inclusion proofs $\pi_i[s_j]$ to the contract. Let $\delta(H_i[s_j], H^*[s_j])$ denote the

numerical deviation from the Inferencer’s committed states. The contract enforces:

$$\text{Slash}(v_i) = \begin{cases} 1, & \text{if } \exists j \text{ s.t. } \delta(H_i[s_j], H^*[s_j]) > \epsilon, \\ 0, & \text{otherwise,} \end{cases} \quad (3)$$

where ϵ is a tolerance threshold capturing floating-point nondeterminism [69], [70]. Verifiers whose openings align with the Inferencer’s states within ϵ receive rewards, while inconsistent openings trigger slashing. To ensure continuous participation, a peer-consistency mechanism statistically compares verifier outputs and rewards correlation with the empirical distribution expected from honest computation, thus discouraging collusion and inactive nodes.

Security under Sampling Majority. Conventional consensus protocols [25], [26] rely on an honest-majority assumption to guarantee safety and liveness. In contrast, VeriLLM achieves correctness under the weaker *one-honest-verifier* (OHV) assumption. Let n denote the total number of verifiers, f the number of malicious ones, and k the committee size for sampling-based verification. The probability that all k selected verifiers are malicious is:

$$P_{\text{fail}} = \frac{\binom{f}{k}}{\binom{n}{k}}. \quad (4)$$

For a fixed corruption rate $\rho = f/n < 0.5$, P_{fail} decreases exponentially in k :

$$P_{\text{fail}} \sim \rho^k, \quad (5)$$

which becomes negligible even for modest committee sizes (e.g., $k = 10$). Thus, VeriLLM maintains strong probabilistic safety guarantees without global replication. To further reduce risk under targeted committee attacks, the system employs a dynamic verifier-selection mechanism that resamples verifiers over epochs, ensuring that adversarial control of a fixed subset cannot persist across rounds. Together with a re-verification fallback procedure, this mechanism ensures that at least one honest verifier detects and reports inconsistencies with overwhelming probability.

5. Protocol Design

5.1. System Overview

VeriLLM is a publicly verifiable, decentralized inference framework for large language models (LLMs) built atop a blockchain substrate. The system aims to achieve three goals simultaneously: (i) correctness that is publicly auditable, (ii) low verification overhead compatible with real-time inference, and (iii) transparent incentive enforcement through smart contracts. To this end, VeriLLM comprises three core components: a *scheduler*, a set of *homogeneous node groups*, and a family of *on-chain verification contracts*. These components collectively coordinate the inference, verification, and reward mechanisms to ensure that every published result is both correct and economically accountable.

- **Scheduler.** The scheduler orchestrates task placement, resource allocation, and verification planning. For each

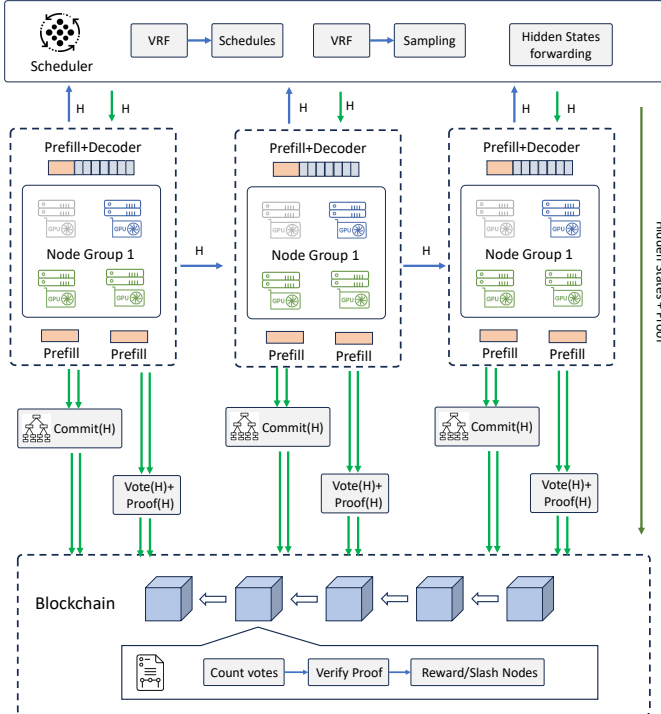


Figure 1. System architecture of VeriLLM. The scheduler employs a verifiable random function (VRF) for unbiased node selection and hidden-state sampling. Each node group performs prefill and decoding, commits hidden states, and submits proofs to the blockchain, which verifies results, counts votes, and applies reward or penalty mechanisms to ensure verifiable decentralized inference.

inference job, it selects a candidate set of node groups capable of jointly executing the model’s layers or tensor partitions. Within each selected group, the scheduler designates one *Inferencer* and several *Verifiers* to handle computation and validation, respectively. Although logically centralized, the scheduler’s randomness and decisions are publicly verifiable: both role assignment and checkpoint sampling derive from a verifiable random function (VRF) [45], producing unpredictable yet reproducible outcomes. This prevents adversaries from precomputing which nodes will be responsible for verification or from biasing verifier selection. The scheduler also records the mapping of job identifiers, selected groups, and Merkle root commitments of intermediate states onto the blockchain for immutable traceability.

• Node Groups. VeriLLM organizes computation across groups of homogeneous GPU workers to simplify performance balancing and state consistency. Each node group corresponds to one or more identical Transformer layers, including all weights, normalization statistics, and kernel parameters. This design aligns with modern distributed inference frameworks such as tensor- and pipeline-parallel architectures [51], [52]. Within a group, a node can serve either as an *Inferencer* or a *Verifier* depending on the scheduler’s role assignment for the current job. To mitigate role-conditioned adversarial strategies, both

roles share a unified execution interface: from the node’s perspective, the input tensor, KV-cache access pattern, and runtime sequence length appear identical for inference and verification. Consequently, at the start of the Prefill phase, a worker cannot distinguish whether it is performing live inference or verifying another node’s computation. This *task-type indistinguishability* provides a built-in security property that limits strategic deviation, since any deviation risks immediate detection if the task later turns out to be a verification probe.

- Verification Contracts.** The verification layer is implemented through on-chain smart contracts [71], [72]. These contracts collect verifier submissions, validate sampling correctness, and finalize verification outcomes through contract-level consensus. Each participating node is required to deposit a stake when registering for inference or verification. The contracts automatically enforce rewards and penalties based on the outcome of verification, slashing misbehaving nodes when inconsistencies or invalid openings are detected. To minimize gas costs, VeriLLM adopts a two-tier protocol: (i) the heavy-lift computation and Merkle proof generation occur off-chain; (ii) only small digests, VRF proofs, and sampled Merkle openings are submitted on-chain. This hybrid design maintains full public verifiability while keeping on-chain cost sublinear in model size. Moreover, the contract interface exposes an event log of all verification transactions, allowing any third-party observer to independently re-verify computations, thereby realizing *trustless auditability*.

Overall, the VeriLLM system model integrates randomness, cryptographic accountability, and economic incentives within a unified architecture. The scheduler enforces randomness and non-manipulability, the node groups ensure hardware-level symmetry and indistinguishability, and the contracts provide immutable verification and incentive enforcement. Together, these elements enable decentralized inference to achieve correctness and efficiency comparable to centralized inference systems, while remaining fully open and publicly verifiable. **End-to-end workflow.** (1) A client submits an inference request to the scheduler, which first selects the node groups that can jointly serve the job and then, using a VRF, chooses one *Inferencer* and several *Verifiers* from each group. (2) The Inferencer executes the forward pass in a pipelined manner, streaming intermediate hidden states to the scheduler; the scheduler records these hidden states and forwards them among inference nodes as needed. (3) After inference completes, the scheduler dispatches the corresponding initial hidden states to the assigned Verifiers. Each Verifier runs a prefill computation to reproduce the target hidden states, compares them with the Inferencer’s hidden states, and submits the comparison result to the smart contract on-chain. (4) To deter “lazy” verification, the scheduler samples hidden-state indices; Verifiers must submit the sampled hidden states for on-chain comparison, and the contract rewards or penalizes Verifiers according to the on-chain outcome.

5.2. Registration

VerILLM employs an on-chain registration mechanism to ensure that all participating entities—both schedulers and worker nodes—are cryptographically identifiable and economically accountable. Registration is enforced through a family of smart contracts that manage collateral, metadata, and state transitions. The process provides two essential guarantees: (i) each participant is uniquely bound to a verifiable cryptographic identity, and (ii) any detected misbehavior can be penalized by slashing its locked stake.

Scheduler registration. Schedulers must register on-chain before they are permitted to coordinate inference tasks. Each registration transaction includes:

- 1) the scheduler’s VRF verification public key, enabling third parties to validate the pseudorandom outputs used in node assignment and hidden-state sampling [45];
- 2) a network endpoint or relay address to facilitate authenticated communication with worker nodes; and
- 3) an initial collateral deposit, ensuring financial accountability for role mismanagement or assignment manipulation.

The VRF key ensures that all sampling and scheduling randomness remains publicly auditable and resistant to pre-computation or selective bias [71], [72].

Node registration. Each worker node must likewise register its model configuration and communication endpoint. The registration payload includes:

- 1) a descriptor of the hosted model m , including architecture identifier and parameter hash, and
- 2) the specific slice ζ of the model it serves (e.g., Transformer layer range, tensor block, or mixture-of-experts shard).

Nodes also deposit a collateral stake that may be forfeited upon evidence of incorrect inference, falsified verification results, or collusion. To ensure fairness and liveness, the registration contract tracks time-stamped updates for all node metadata, allowing the scheduler to continuously maintain an up-to-date view of system membership.

Withdrawal and penalties. Registered entities may deregister and reclaim their stake, but withdrawals are subject to a fixed unbonding period Δ_{wait} . This grace interval ensures that any pending disputes or verification results can still trigger penalties before funds are released. Let t_{dereg} denote the deregistration timestamp. A withdrawal is finalized only after $t_{\text{final}} = t_{\text{dereg}} + \Delta_{\text{wait}}$, ensuring causal closure of all ongoing verifications.

This mechanism parallels the delayed-withdrawal model of accountable distributed systems [25], [73], guaranteeing that both schedulers and workers remain economically bound to their past behavior.

5.3. Scheduling Scheme

The Scheduler coordinates node selection and hidden-state (HS) forwarding across a pipeline of model slices, ensuring efficient inference and verifiable parallelism. While

logically centralized for low-latency operation, all scheduling decisions are derived from verifiable randomness to prevent manipulation or bias.

Verifiable randomness and auditability. Each scheduling decision is deterministically derived from a publicly verifiable random beacon instantiated via a verifiable random function (VRF) [45]. The Scheduler’s VRF verification key is registered on-chain, and every scheduling round includes the tuple:

$$(\text{job_id}, \text{VRF_out}, \text{VRF_proof}), \quad (6)$$

where VRF_out encodes the pseudorandom seed used for node assignment and hidden-state sampling, and VRF_proof allows any observer or contract to independently validate correctness. This construction guarantees that role assignment and verification checkpoints are unpredictable yet verifiable, preventing any party from biasing job allocation.

Node state maintenance. The Scheduler maintains a continuously updated view of the network’s active nodes by monitoring on-chain registration events. Let \mathcal{N} denote the global set of registered nodes. Each node $n \in \mathcal{N}$ exposes metadata fields $\text{model}(n)$ and $\text{slice}(n)$, describing its hosted model and layer range, respectively. The Scheduler constructs homogeneous groups as:

$$G_{m,\zeta} = \{n \in \mathcal{N} \mid \text{model}(n) = m, \text{slice}(n) = \zeta\}, \quad (7)$$

where each group represents a cohort of workers hosting identical model slices. For a model m with L slices, the pipeline composition is:

$$\mathcal{P}(m) = \langle G_{m,1}, G_{m,2}, \dots, G_{m,L} \rangle. \quad (8)$$

When serving a new inference request for model m , the Scheduler randomly selects one *Inferencer* and k *Verifiers* within each group $G_{m,\zeta}$ using the VRF seed. The assignments are thus both deterministic (given the VRF output) and unpredictable (prior to seed revelation).

Latency and flow control. The Scheduler coordinates hidden-state (HS) forwarding between consecutive groups. Let T_ζ denote the transmission latency between $G_{m,\zeta}$ and $G_{m,\zeta+1}$. The expected end-to-end latency T_{total} for an L -slice pipeline is:

$$T_{\text{total}} = \sum_{\zeta=1}^L (T_\zeta + T_{\text{compute}}^{(\zeta)}), \quad (9)$$

where $T_{\text{compute}}^{(\zeta)}$ is the average inference time per slice. Because role assignment is randomized per job, load balancing is implicitly achieved, reducing variance in $T_{\text{compute}}^{(\zeta)}$. This property ensures that verification and inference remain tightly coupled without imposing additional synchronization barriers.

In summary, the Scheduler functions as a lightweight but verifiably accountable control plane: it ensures transparent randomness, deterministic scheduling, and reproducible verifier selection, all while preserving the performance characteristics of centralized inference.

5.4. Task Scheduling and Hidden-State Management

Task Scheduling. Upon receiving a user request req , the Scheduler identifies a sequence of node groups $\langle G_{m,1}, G_{m,2}, \dots, G_{m,L} \rangle$ that collectively host the model segments required to execute the target model m . Each group G_i comprises $L_i = |G_i|$ homogeneous nodes, each storing an identical slice of the model parameters and runtime configuration. To ensure that role assignment is unpredictable yet publicly auditable, the Scheduler derives a per-stage random seed using a verifiable random function (VRF) bound to the request hash, stage index, and group cardinality:

$$h \leftarrow H(\text{req}), \quad r_i \leftarrow \text{VRF}(sk_{\text{sch}}, h, i, L_i), \quad (10)$$

where sk_{sch} is the Scheduler's VRF secret key, and the corresponding verification key vk_{sch} is recorded on-chain. The Scheduler publishes (r_i, π_i) , where π_i is the VRF proof that allows any observer to validate:

$$\text{VRF.Verify}(vk_{\text{sch}}, \langle h, i, L_i \rangle, r_i, \pi_i) = 1. \quad (11)$$

The seed r_i initializes a cryptographically secure pseudorandom number generator (CSPRNG), such as a Fisher–Yates permutation seeded with $\text{HKDF}(r_i)$, producing an unbi- asable permutation σ_i over the node indices in G_i . From this permutation, the Scheduler deterministically assigns one *Inferencer* and k *Verifiers*:

$$n_i^{\text{inf}} = G_{m,i}[\sigma_i(1)], \quad \{n_{i,1}^{\text{ver}}, \dots, n_{i,k}^{\text{ver}}\} = G_{m,i}[\sigma_i(2..k+1)]. \quad (12)$$

Because each seed r_i is cryptographically bound to (h, i, L_i) and its proof is anchored on-chain, the resulting assignments are verifiable, reproducible, and non-manipulable. Any deviation by the Scheduler or a colluding node is thus immediately detectable through public audit.

Hidden-State Forwarding. Once role assignment is finalized, the Scheduler coordinates distributed inference as a pipelined relay across the L model segments. Let t denote the current decoding step. At each step, the pipeline executes as follows:

- 1) The Scheduler transmits the active token sequence \mathbf{y}_t (with \mathbf{y}_1 as the initial prompt) to the first segment's Inferencer ($i = 1$). This node computes its hosted layers to produce the hidden-state tensor $S_2^{(t)}$.
- 2) The Scheduler forwards $S_2^{(t)}$ to the next Inferencer ($i = 2$), which computes $S_3^{(t)}$, and so on through the pipeline.
- 3) The relay proceeds until the final Inferencer ($i = L$) produces the terminal hidden state $S_{L+1}^{(t)}$, evaluates the output logits, and predicts the next token y_{t+1} , which is returned to the Scheduler.
- 4) The Scheduler delivers y_{t+1} to the user and re-injects it as input for the next iteration ($t \leftarrow t + 1$).

The loop terminates when $y_t = \langle \text{EOS} \rangle$. This hop-by-hop relay architecture enables fine-grained auditing and fault isolation while maintaining end-to-end latency comparable

to centralized inference. Each intermediate tensor $S_i^{(t)}$ is checkpointed for potential verification, ensuring deterministic reproducibility without interrupting the decoding stream.

During each decoding iteration t , the overall pipeline computation proceeds as follows. The Scheduler receives the current token sequence \mathbf{y}_t (where $t=1$ corresponds to the prompt) and forwards it to the first segment's Inferencer. The first segment embeds and processes $\mathbf{y}_{<t}$ to produce the intermediate hidden state:

$$S_2^{(t)} = g_1(\text{Embed}(\mathbf{y}_{<t})). \quad (13)$$

Each subsequent segment $i = 2, \dots, L$ receives the preceding output $S_i^{(t)}$, executes its corresponding model layers, and produces:

$$S_{i+1}^{(t)} = g_i(S_i^{(t)}). \quad (14)$$

At the final stage, the tail segment computes the logits and predicts the next token:

$$y_{t+1} = \arg \max f_{\text{LM}}(S_{L+1}^{(t)}). \quad (15)$$

The newly generated token y_{t+1} is then appended to the existing sequence, forming $\mathbf{y}_{\leq t} = \mathbf{y}_{<t} \| y_t$, which is passed back to the first segment to initiate the next decoding step. If $y_t = \langle \text{EOS} \rangle$, the inference process halts.

Hidden-State Logging and Commitment. To enable verifiable post-hoc auditing, each Inferencer logs its intermediate hidden states for every token and commits to them using cryptographic proofs. For each token index t , an Inferencer serializes its output tensor $S_i^{(t)} \in \mathbb{R}^{d_k \times d_v}$, constructs a Merkle tree $\text{Merkle}(S_i^{(t)})$ over all scalar entries, and submits the Merkle root $\gamma_i^{(t)}$ accompanied by a bound signature:

$$\text{Sig}_{\text{inf}}(h, i, t, \gamma_i^{(t)}). \quad (16)$$

To prevent tampering or substitution during relay, the Scheduler also signs the forwarded root:

$$\text{Sig}_{\text{sch}}(h, i, t, \gamma_i^{(t)}), \quad (17)$$

ensuring accountability for both the producer and the forwarder. This dual-signature commitment model provides end-to-end traceability: any discrepancy between a segment's output and the forwarded record can be attributed with cryptographic certainty. Because verifiers only require Merkle openings for sampled positions, the bandwidth and on-chain verification costs scale sublinearly with tensor size. The integration of deterministic serialization, Merkle-based commitment [44], and chained signatures provides tamper-evident provenance for all hidden states without introducing measurable latency into the inference path.

Overall, this architecture ensures that every stage of distributed inference remains cryptographically auditable while preserving throughput and latency comparable to optimized large-model serving systems [51], [52].

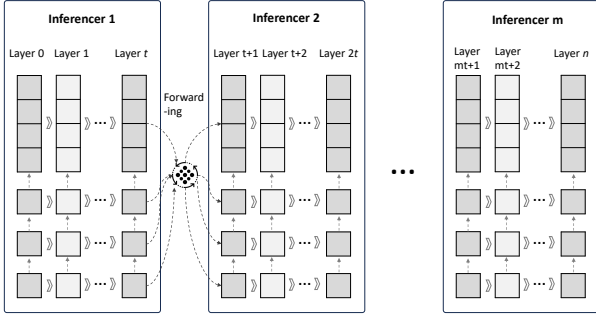


Figure 2. Overview of the decentralized inference architecture. Each segment hosts identical Transformer layers, and hidden states are relayed across the pipeline under cryptographic commitments.

5.5. Inference Scheme

The inference process executes online, autoregressive generation over a decentralized, pipelined fabric of homogeneous node groups. Each group hosts an identical copy of a contiguous Transformer block, including weights, normalization statistics, and kernel configurations [51], [52]. For each incoming task, the Scheduler selects eligible groups and, through a verifiable random function (VRF) [45], assigns one *Inferencer* per group to execute the live forward pass. Verifier roles are simultaneously drawn from the same VRF distribution but remain inactive during this phase. Throughout generation, the Scheduler relays and logs hidden states across segment boundaries, appending cryptographic commitments and signatures to construct an auditable trace that serves as the foundation for subsequent verification [27], [38].

Formally, let the model be divided into L contiguous segments. At decoding step t , given the causal input $x_{1:t} = [\text{prompt} \| y_{1:t-1}]$, each segment computes its portion of the forward pass as follows:

$$S_1^{(t)} \leftarrow \text{Embed}(x_{1:t}), \quad (18)$$

$$S_{i+1}^{(t)} \leftarrow F_i(S_i^{(t)}; W_i), \quad i = 1, \dots, L, \quad (19)$$

$$y_t \leftarrow \text{Decode}(S_{L+1}^{(t)}), \quad (20)$$

where $S_i^{(t)}$ is the hidden state entering segment i , F_i denotes the segment's forward operator, W_i its parameters, and Decode the final output head combined with the sampling rule. The resulting pipeline achieves token-serial yet segment-parallel execution, synchronized by the Scheduler's relay of hidden states [51].

Scheduler-Driven Role Assignment. For each inference task, the Scheduler enumerates all node groups capable of collectively serving the model and assigns roles in a publicly verifiable manner. Using a VRF bound to the task identifier [45], it deterministically selects one Inferencer per group, while keeping the randomness unpredictable before the VRF proof is revealed. This mechanism ensures that role assignment cannot be biased or precomputed and that every selection remains verifiable through the VRF proof posted on-chain [40], [50].

Pipelined Forward and State Relay. During decoding step t , segment i 's Inferencer receives from the Scheduler both the upstream hidden state $S_i^{(t)}$ and a tamper-evidence package containing a commitment to $S_i^{(t)}$ and a proof of authenticity from the previous node. The Inferencer then:

- 1) performs the forward pass to produce $S_{i+1}^{(t)}$;
- 2) computes a cryptographic commitment to $S_{i+1}^{(t)}$ (e.g., a Merkle root over a deterministic serialization [44]) and signs the root with its node key; and
- 3) returns the tuple $\{S_{i+1}^{(t)}, \text{root}_i^{(t)}, \sigma_i^{(t)}\}$ to the Scheduler.

The Scheduler verifies each signature against the on-chain registry (optionally through a zero-knowledge membership proof [38], [39] to preserve role anonymity), appends its own relay signature, persists the state to stable storage, and forwards the package to the next segment's Inferencer. To minimize latency, each receiving node can begin its computation immediately while performing signature verification asynchronously; if any proof later fails, the Scheduler aborts the affected pipeline and invalidates dependent results.

Commitment and Signature Discipline. At every token step and segment boundary, the produced hidden state is cryptographically anchored by:

- 1) a commitment $\text{root}_i^{(t)} = \text{MerkleRoot}(S_{i+1}^{(t)})$, and
- 2) a node signature $\sigma_i^{(t)} = \text{Sig}(\text{sk}_i, \text{root}_i^{(t)})$.

All node public keys are registered under an on-chain Merkle accumulator, enabling compact membership proofs [45], [50]. Instead of forwarding raw signatures, the Scheduler may alternatively issue a zero-knowledge proof attesting that it holds a valid signature from some registered key on the advertised root—thereby maintaining verifiability without revealing node identity [39], [40]. Each forwarded artifact is re-signed by the Scheduler to guarantee origin authenticity and replay protection. This layered commitment and signature discipline ensures that every hop in the relay chain is both tamper-evident and cryptographically attributable.

Autoregressive Token Emission and Feedback. The terminal segment ($i = L$) outputs logits or the final hidden state for token t , from which the next token y_t is sampled according to the decoding policy [2]. The Scheduler collects y_t and feeds it back into the pipeline to form $x_{1:t+1}$, advancing the process to step $t+1$. The loop continues until the model emits an end-of-sequence token $\langle \text{EOS} \rangle$ or another termination condition is met.

Task-Type Indistinguishability and Robustness. The communication protocol, message format, and API surface used by Inferencers during inference are identical to those used by Verifiers in the subsequent verification phase [11]. Consequently, no node can distinguish in real time whether it is performing live inference or participating in a verification probe. This indistinguishability eliminates the opportunity for strategic deviation and simplifies implementation symmetry across both phases. Combined with VRF-driven role assignment, signed commitments, and auditable relays,

the inference scheme produces a verifiable, tamper-evident execution trace with negligible online overhead.

5.6. Verification Scheme

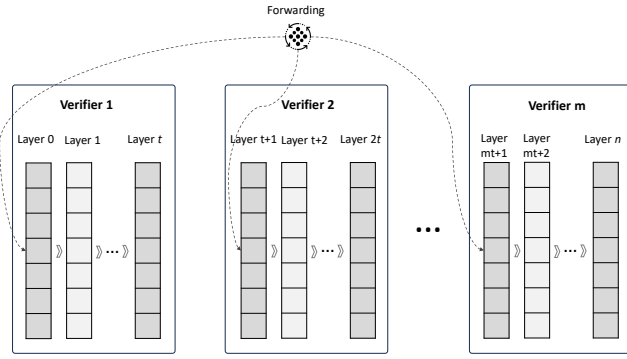


Figure 3. Overview of the decentralized verification architecture. Each verifier independently reconstructs its segment’s outputs via a full-sequence prefill, comparing committed and recomputed states.

During autoregressive inference, an LLM executes two phases: a *prefill* pass—where the prompt tokens are processed in parallel to populate the key–value (KV) cache—and a *decode* phase—where tokens are generated sequentially with causal dependencies on all previous outputs [2], [52]. The decoding phase dominates latency and is inherently serial, leading to limited GPU utilization and memory-bound performance [51]. However, verification differs fundamentally: once the full output sequence $y_{1:T}$ is known, the verifier is no longer constrained by sequential dependencies. Instead, it can recompute all token representations simultaneously under the same causal mask, yielding a single parallel pass equivalent to prefill over the concatenated prompt–output sequence [27], [39].

Formally, let the input to the verifier be the complete sequence

$$x = [\text{prompt} \| y_{1:T}], \quad (21)$$

and let $\mathcal{S} = [S^{\text{prompt}} \| S^1 \| \dots \| S^T]$ denote the concatenated hidden states across all positions. Given the causal structure of the Transformer, the verifier can execute a single forward pass to reconstruct all hidden states $\{S_i^{(t)}\}_{t=1}^T$ for every segment $i \in [1, L]$ without performing incremental token decoding [74]. This transformation replaces T serial decode iterations with a single batched forward computation, eliminating redundant KV-cache updates and reducing cross-node communication. In practice, this yields significantly improved GPU utilization, especially on architectures with high Tensor Core throughput [51].

Because the Scheduler has recorded the hidden states produced by each inferencer at every segment boundary, each verifier can recompute its designated segment locally. Specifically, for segment i , the verifier uses the recorded upstream hidden states $\{S_i^{(t)}\}_{t=1}^T$ as its inputs and executes only its own block of layers to regenerate $\{S_{i+1}^{(t)}\}_{t=1}^T$. This

independence allows all L verifiers to run concurrently across the distributed network, each responsible for validating one contiguous model partition. Assuming near-uniform load balance and negligible orchestration or I/O overhead, the total wall-clock verification time satisfies

$$T_{\text{verify}} \approx \frac{1}{L} T_{\text{prefill}}(\text{full model}), \quad (22)$$

yielding near-linear scaling in the number of participating verifier groups [27], [51].

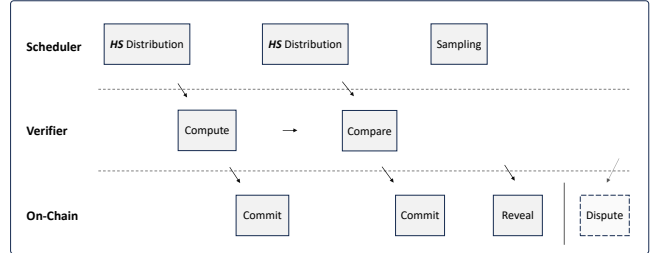


Figure 4. Verification workflow. Each verifier independently executes a full-sequence prefill over its model segment and commits its output root to the blockchain for later consistency checks.

Prefill Computation. After the inference phase concludes, the Scheduler initiates segment-local verification by distributing the required input states to each verifier [40]. For segment $i > 1$, the Scheduler sends the sequence $\{S_i^{(t)}\}_{t=1}^T$ —the hidden states produced by the upstream inferencer for all tokens. For the first segment ($i = 1$), the Scheduler instead provides the full tokenized input $[\text{prompt} \| y_{1:T}]$, corresponding to the raw embedding input of the model. Upon receipt, each verifier executes a full-sequence prefill limited to its hosted layers:

$$S_{i+1}^{(t)} = F_i(S_i^{(t)}; W_i), \quad \forall t \in [1, T], \quad (23)$$

where F_i denotes the forward mapping of segment i and W_i its parameters.

Importantly, the communication interface, data serialization format, and RPC protocol used during verification are identical to those used in live inference [11]. This design choice enforces *task-type indistinguishability*: from the perspective of any node, it is impossible to discern whether the current request corresponds to live inference or a verification probe [50]. Such indistinguishability eliminates mode-specific behavior and prevents nodes from selectively deviating or shortcircuiting computation when acting as verifiers. Upon completion, each verifier must return its computed outputs $\{S_{i+1}^{(t)}\}_{t=1}^T$ through the same interface as during inference, producing an auditable trace indistinguishable in structure and timing.

Commitment Submission. Once the local recomputation completes, the Scheduler transitions verifiers into the commit phase. Each verifier constructs a tamper-evident cryptographic commitment to its final outputs—specifically, the hidden state corresponding to the last token ($t = T$) at its

segment's output boundary. This commitment is instantiated as a Merkle root [44]:

$$\text{root}_i^{(T)} = \text{MerkleRoot}(S_{i+1}^{(T)}), \quad (24)$$

built over a canonical serialization of the tensor with scalar elements as leaves. The verifier then signs this root with its registered key:

$$\sigma_i^{(T)} = \text{Sig}(\text{sk}_i, \text{root}_i^{(T)}), \quad (25)$$

and publishes the commitment on-chain through the designated verification contract [38], [39].

This on-chain record provides a permanent anchor for later verification steps. In subsequent sampling or dispute phases, verifiers may be required to disclose specific slices or elements of the hidden state $\{S_{i+1}^{(T)}\}$, accompanied by Merkle inclusion proofs that can be efficiently checked against the posted root [45], [50]. This approach ensures both compactness and auditability: the entire verification process involves only lightweight commitments and selective disclosures rather than full tensor uploads, keeping blockchain overhead minimal while preserving cryptographic integrity.

In summary, the verification scheme leverages the known output sequence and the pre-recorded intermediate states to convert sequential autoregressive computation into parallel, segment-local prefill verification. Combined with Merkle commitments and signature anchoring, this design achieves strong verifiability and high throughput, ensuring that even a single honest verifier can detect and prove any inference deviation with overwhelming probability [39], [40].

5.7. Comparison, Sampling, and On-Chain Adjudication

Comparison and On-Chain Commitment. After all designated verifiers have posted their commitments (or the commitment deadline expires), the Scheduler distributes, off-chain, the inferencer-produced target hidden states $\{S_i^{(t)}\}_{t=1}^T$ for the relevant segment i to each verifier assigned to that segment. Each verifier v recomputes its local segment to obtain $\{\hat{S}_i^{(t)}\}_{t=1}^T$ and computes elementwise discrepancies $\Delta^{(t)} = \hat{S}_i^{(t)} - S_i^{(t)}$. Let $\phi(\cdot)$ denote a scalar aggregation function such as mean absolute error, and $\Psi(\cdot)$ a statistic (mean or clipped mean) summarizing deviations across tokens. The resulting score $T_v = \Psi(\{\phi(\Delta^{(t)})\}_{t=1}^T)$ is compared against a tolerance τ calibrated for floating-point nondeterminism [51]. The verifier's binary verdict is

$$b = \mathbb{I}[T_v \leq \tau] \in \{0, 1\}. \quad (26)$$

To prevent adaptive or copy-cat reporting, the verifier posts a hiding, binding commitment

$$C = \text{Commit}(b, r), \quad (27)$$

where r is fresh randomness; C is posted during the commit phase, and (b, r) is revealed later [27], [50].

Data Sampling. To ensure verifiers actually perform computation, the contract performs on-chain spot checks of sampled tensor elements [38], [45]. Once verdict commitments are posted, the Scheduler uses a verifiable random function (VRF) to generate unbiased sample indices:

$$(r_i, \pi_i) \leftarrow \text{VRF.Eval}(sk_{\text{sch}}, \langle h, i, \{\gamma_j\}_{j=1}^m \rangle), \quad (28)$$

$$\mathcal{T}_i \leftarrow \text{Sample}(\text{HKDF}(r_i); n, q), \quad (29)$$

where h is the task hash, $\{\gamma_j\}$ the posted Merkle roots, n the sample size, and q a stratification policy.

The Scheduler then publishes:

$$\langle r_i, \pi_i, \mathcal{T}_i, \mathbf{V}_{\mathcal{T}_i}^{(T)}, \gamma_{i,\text{inf}}^{(T)}, \text{Sig}_{i,\text{inf}}^{(T)}, \{\text{MP}_j^{\text{inf}}\}_{j \in \mathcal{T}_i} \rangle, \quad (30)$$

where $\mathbf{V}_{\mathcal{T}_i}^{(T)}$ are reference values, $\gamma_{i,\text{inf}}^{(T)}$ is the inferencer's root, and MP_j^{inf} are Merkle proofs. The contract enforces three checks:

1) VRF validity:

$$\text{VRF.Verify}(vk_{\text{sch}}, \langle h, i, \{\gamma_j\} \rangle, r_i, \pi_i) = 1; \quad (31)$$

2) Origin authenticity:

$$\text{VerifySig}(\text{pk}_{i,\text{inf}}, \gamma_{i,\text{inf}}^{(T)}, \text{Sig}_{i,\text{inf}}^{(T)}) = 1; \quad (32)$$

3) Inclusion correctness:

$$\forall j \in \mathcal{T}_i, \text{MerkleVerify}(\gamma_{i,\text{inf}}^{(T)}, \mathbf{V}_j^{(T)}, \text{MP}_j^{\text{inf}}) = 1. \quad (33)$$

These checks guarantee unbiased sampling, authentic roots, and valid inclusion proofs [44]. Any mismatch can be publicly demonstrated with the Scheduler's relay signatures, triggering immediate slashing.

Reveal. Each verifier opens its commitment and provides sampled entries $\{v_j\}_{j \in \mathcal{T}_i}$ with Merkle proofs $\{\text{MP}_j^{\text{ver}}\}$:

(1) Commitment opening:

$$\text{OpenCommit}(C; b, r) = 1; \quad (34)$$

(2) Merkle inclusion:

$$\forall j \in \mathcal{T}_i, \text{MerkleVerify}(\gamma_{i,\text{ver}}^{(T)}, v_j, \text{MP}_j^{\text{ver}}) = 1; \quad (35)$$

(3) Value matching:

$$\Delta_j = |v_j - \mathbf{V}_j^{(T)}| \leq \varepsilon, \quad (36)$$

where ε captures tolerated numeric noise [51]. The agreement rate

$$\hat{p} = \frac{1}{|\mathcal{T}_i|} \sum_{j \in \mathcal{T}_i} \mathbb{I}[\Delta_j \leq \varepsilon] \quad (37)$$

must satisfy $\hat{p} \geq \theta$ for a positive verdict $b = 1$.

Tail verifiers ($i = L$) perform an additional token-consistency check [2]:

$$\text{TokenMatch}(\arg \max f_{\text{LM}}(S_{L+1}^{(T)}), y_T) = 1, \quad (38)$$

ensuring that the recomputed logits correspond to the reported output token.

Detection Probability and Parameterization. Let α denote the per-sample error rate when computation is incorrect. With n sampled entries,

$$P_{\text{pass}} \leq (1 - \alpha)^n, \quad (39)$$

so to bound undetected cheating by δ ,

$$n \geq \frac{1}{\alpha} \ln \frac{1}{\delta}. \quad (40)$$

Calibration experiments provide empirical lower bounds on α and guide the choice of ε and θ , balancing tolerance and sensitivity [39].

On-Chain Adjudication. After reveal, the contract aggregates revealed verdicts $\{b_v\}_{v \in V}$ from m verifiers. If a majority agree ($B \geq m/2$), the inference is accepted and honest verifiers share rewards. If most disagree but maintain internal consistency (pairwise hidden-state deviation $\leq \varepsilon$ over at least a τ -fraction of pairs), the negative verdict stands and consistent verifiers are rewarded. Otherwise, the outcome is indeterminate; any verifier may later submit a succinct zero-knowledge proof demonstrating an error, triggering inferencer slashing and bounty payout [38], [40].

Overall, the protocol combines VRF-based unbiased sampling, Merkle commitments, and commit-reveal sequencing into a scalable, probabilistically sound verification mechanism. It provides high fraud-detection probability at cost proportional to sample size n , not tensor dimensionality, achieving secure, low-overhead verification in decentralized LLM inference systems.

Dispute Resolution. The above mechanism guarantees correctness under a one-honest-verifier assumption but also supports escalation when committee capture is suspected. Because each verification task samples only a small committee ($m \ll N$), an adversary controlling a modest network fraction may occasionally dominate a sampled group. To mitigate this risk, if the first-round verdict is negative, the inferencer may request a *reverification* with an expanded committee of size $m' > m$. If the second-round majority produces a positive outcome, the contract rescinds the inferencer's penalty and slashes all first-round verifiers who voted False. Conversely, if the extended committee upholds the negative verdict, the inferencer bears the cost of the additional round.

This multi-stage design achieves *adaptive robustness*: typical cases finalize in one verification round with minimal on-chain load, while disputed cases escalate probabilistically until resolved with high confidence [38], [50].

6. Security Analysis

6.1. Threat Model and Assumptions

VeriLLM operates in a decentralized and adversarial environment where participants may deviate arbitrarily from the protocol to reduce computation cost or bias outcomes. We consider three potentially malicious roles—*Inferencers*, *Verifiers*, and a partially trusted or even Byzantine *Scheduler*. Smart contracts execute deterministically as deployed

and are assumed correct by construction [50]. The security goal is to guarantee inference correctness and accountability under these adversarial conditions.

Cryptographic assumptions.. VeriLLM relies on standard primitives with the following properties:

- **EUF-CMA security of digital signatures.** Node signatures are existentially unforgeable under chosen-message attack, preventing impersonation or undetected alteration of signed artifacts [45].
- **Collision resistance of hash functions and binding of Merkle commitments.** Once a node publishes a Merkle root γ , no two distinct tensors can produce the same root, ensuring immutability of hidden-state logs [44].
- **Unbiased verifiable randomness.** VRF outputs used for role assignment and sampling are unpredictable prior to evaluation and publicly verifiable afterward, precluding adaptive bias [45].
- **Soundness of zero-knowledge proofs.** When zero-knowledge proofs attest signature validity or batched inclusion proofs, any false statement is rejected except with negligible probability [38], [39].

System assumptions.. Beyond cryptographic foundations, the protocol assumes realistic system conditions:

- **One-honest-verifier assumption.** At least one verifier per task is honest and online. This weaker-than-majority assumption suffices to guarantee safety via full re-execution or sampled audit detection [27].
- **Eventual synchrony.** The network eventually delivers all messages. Smart contracts enforce timeouts and a commit-then-reveal order to prevent adaptive inference of partial states.
- **Bounded numeric nondeterminism.** Hardware and kernel-induced floating-point variance is modeled as small zero-mean noise within threshold ε ; honest executions pass with overwhelming probability [51].

These assumptions align with the threat model of verifiable ML systems such as zkML [38], zkLLM [39], and decentralized inference frameworks [15], [41].

6.2. Security Objectives

VeriLLM provides cryptographically auditable correctness guarantees for large-scale LLM inference with minimal overhead. When all nodes behave honestly, both the off-chain and on-chain verification phases accept except with negligible probability due to benign numeric noise. If an Inferencer produces an incorrect result—by pruning layers, quantizing weights, truncating decoding, or recycling stale states—then one of three independent mechanisms detects it: (i) full hidden-state recomputation, (ii) commit-then-sample audit enforcing random openings, or (iii) a zero-knowledge proof of inconsistency from an honest verifier [40]. Thus, any materially incorrect inference is provably detectable on chain.

Trace integrity. Every hidden-state tensor exchanged between segments is bound by a Merkle root γ and node signature. The Scheduler re-signs each relay, so tampering,

omission, or reordering requires forging a valid signature or producing inconsistent Merkle openings—computationally infeasible under our assumptions.

Unpredictable sampling. Sampling indices for audits are derived from VRF outputs computed after all commitments are posted, eliminating adaptivity and ensuring independence between commitments and revealed indices [45].

Task-type indistinguishability. Inferencers and Verifiers use identical RPC interfaces and serialization formats. Nodes cannot determine whether a request is for live inference or verification, removing the incentive for selective deviation or strategic laziness.

6.3. Commit–Then–Sample: Binding and Unpredictability

The commit–then–sample protocol underpins VeriLLM’s verifiability. Each node first commits to its hidden-state tensor via Merkle root r_i ; after all roots are posted, a public seed

$$R = \text{Hash}(r_1, r_2, \dots, r_n) \quad (41)$$

is computed to derive sampling positions. This sequencing guarantees both *binding* (immutability) and *unpredictability* (fair randomness).

Lemma 1 (Binding). *Given a collision-resistant hash and a binding Merkle tree, a prover that posts r_i cannot later open inconsistent values at any sampled index except with negligible probability.*

Lemma 2 (Unpredictability). *If $R = \text{Hash}(r_1, \dots, r_n)$ is computed only after all roots are posted, and the hash is modeled as a random oracle, then sampling indices are computationally unpredictable to any participant at commit time.*

Together, these properties ensure that a node committing to falsified or incomplete states cannot anticipate future audits and will be detected with overwhelming probability. This commit–then–sample discipline yields deterministic accountability and makes deviation economically irrational in expectation [27], [38].

6.4. Analysis of Concrete Attacks

We analyze representative adversarial strategies against VeriLLM and show that each is provably detected or economically disincentivized under the stated assumptions. The analysis covers both model-level deviations and protocol-level cheating behaviors.

6.4.1. Quantization Attack. An Inferencer executes a quantized variant of the prescribed model (e.g., W8A8 precision) to reduce computation and memory cost while claiming compliance with the full-precision configuration. Quantization alters rounding distributions and mantissa statistics, introducing systematic deviations across hidden states and logits that may be small per position but accumulate over long sequences.

Defenses. (i) *Offline full-sequence recomputation.* Each verifier recomputes its assigned segment on the complete sequence and performs hypothesis tests over hidden-state statistics sensitive to precision drift. Let $S_{i+1}^{(t)}$ denote the inferencer’s state and $\hat{S}_{i+1}^{(t)}$ the verifier’s recomputation. Elementwise deviations $\Delta^{(t)} = \hat{S}_{i+1}^{(t)} - S_{i+1}^{(t)}$ feed a battery of tests T_{off} such as

$$\begin{aligned} P_{\text{exp}} &= \frac{1}{N} \sum \mathbb{I}[\exp(\hat{S}) \neq \exp(S)], & Q_{\text{small}} &= \frac{1}{N} \sum \mathbb{I}[|\Delta| \leq 10^{-5}], \\ Z_{\text{large}} &= \frac{1}{N} \sum \mathbb{I}[|\Delta| > \tau_{\text{large}}], & \text{MAE} &= \frac{1}{N} \sum |\Delta|. \end{aligned} \quad (42)$$

Thresholds are calibrated from benign full-precision runs. Honest executions pass T_{off} with probability $1 - \text{negl}(\lambda)$, whereas 8-bit quantization causes detectable statistical shifts. (ii) *Lightweight on-chain spot check.* The contract performs a relaxed test T_{on} on VRF-sampled final-token scalars, checking $|v_j - \mathbf{V}_j^{(T)}| \leq \varepsilon$ and aggregating agreement against a threshold θ [38]. This sustains liveness while bounding on-chain cost to $O(n)$ sampled entries.

Security claim. With thresholds derived from calibration and sample size $n \geq \frac{1}{\alpha} \ln(1/\delta)$, the false-acceptance probability for a quantized model is negligible in sequence length and dimension, while honest runs maintain service-level accuracy.

6.4.2. Early-Termination Attack. **Attack.** The Inferencer prematurely halts decoding before emitting $\langle \text{EOS} \rangle$, fabricating terminal states or tokens to save computation.

Defenses. (i) *Tail-token consistency.* The last-segment verifier recomputes logits from the reported final hidden state and verifies that the decoding policy yields the claimed token [27]. Any premature termination produces a mismatch at the tail step with probability 1 for deterministic decoding and with high probability for deterministically reseeded stochastic decoding. (ii) *Per-step binding.* Each segment’s boundary state is individually committed and signed. Modifying terminal states or inserting fake tokens requires forging a signature or producing an inconsistent Merkle opening, both computationally infeasible [44], [45]. Scheduler relay signatures bind token order and prevent state splicing.

Security claim. Premature termination necessarily triggers token- or commitment-level inconsistency and is detected with overwhelming probability.

6.4.3. Forged Output via Small Model. Attack. An adversary uses a smaller model to generate a cheap surrogate sequence \tilde{y} and runs a single full-sequence prefill on the large model with $[\text{prompt} \parallel \tilde{y}]$ to produce superficially coherent hidden states, avoiding the true decoding loop.

Defenses. (i) *Token-state cross-check.* Verifiers decode from recomputed last-layer states and compare predicted tokens with the inferencer’s outputs. Unless $\tilde{y} = y^*$ (the true decode of the prescribed model), token mismatches occur at multiple checked positions with overwhelming probability. (ii) *Transcript continuity.* The scheduler enforces that each step’s input to segment 1 equals $[\text{prompt} \parallel y_{1:t}]$ carried from previous steps. Relay signatures and Merkle openings

cryptographically bind tokens and hidden states into a single ordered transcript, making replacement of \tilde{y} infeasible.

Security claim. Except for negligible coincidence where \tilde{y} exactly matches y^* , the forged-output attack fails due to token-state inconsistency revealed by sampled checks.

6.4.4. Lazy Verifier (Free-Riding). Attack. A verifier omits local prefill, posts an arbitrary acceptance verdict, and relies on others’ honesty to collect rewards undetected.

Defenses. (i) *Commit-then-open discipline.* Before seeing sampling indices, each verifier must commit to its final-token tensor root and later open VRF-selected positions with inclusion proofs [45]. Without genuine computation, the probability of producing valid openings is negligible. (ii) *Task-type indistinguishability.* Because inference and verification share identical RPC interfaces and data formats, workers cannot distinguish verification probes from live inference [27], preventing selective laziness. (iii) *Reward gating.* Rewards are paid only to verifiers whose openings pass on-chain checks; mismatches or failures trigger stake slashing. Hence, skipping computation is a strictly dominated strategy.

Security claim. Given Merkle binding and unpredictable VRF sampling, a non-computing verifier cannot produce correct openings except with negligible probability and is penalized accordingly.

6.5. Collusion, Censorship, and Dispute

Collusion among verifiers. A coalition may attempt to fabricate mutually consistent hidden states and corresponding Merkle roots such that on-chain openings match internally forged commitments. The commit-then-sample discipline prevents any *post hoc* adaptation: once a root is posted, the coalition must open VRF-chosen indices consistent with that fixed root. To ensure semantic correctness with respect to the prescribed model, VeriLLM introduces two safeguards: (i) *token-state cross-checks* at the tail segment, where verifiers decode from recomputed last-layer states and compare tokens to the published outputs; and (ii) a *zero-knowledge escalation path*, in which any single honest verifier can submit a succinct proof that a challenged prefix of the transcript violates the model’s forward mapping or decoding rule [38], [39], [40]. The contract verifies the proof on-chain, finalizing the inconsistency independently of the coalition’s reports.

Scheduler misbehavior. The Scheduler cannot modify hidden states without forging a node signature or producing an invalid membership proof for the signer set maintained on-chain. Selective exclusion or biased role assignment is publicly detectable: once (r, π) pairs are published, anyone can recompute the VRF output and compare it to the Scheduler’s assignment. Any mismatch deterministically identifies the deviation and triggers stake slashing.

Censorship resistance. All commitments are recorded on-chain, and verifier selection derives from verifiable randomness. To suppress detection, an adversary would need to corrupt or block all selected verifiers for a task. Under the

one-honest-verifier assumption, at least one remains live to perform offline recomputation, pass the sampled checks, or post a zero-knowledge inconsistency proof. A total denial of service is observable through missed deadlines, which activate timeout-based remediation.

6.6. Completeness and Soundness Summary

Let \mathcal{E} denote the event that an incorrect inference passes all checks.

Soundness. If the Inferencer deviates from the prescribed execution—through quantization, truncation, or forged outputs—then one of the following mechanisms detects the deviation with overwhelming probability: (i) full-sequence recomputation with calibrated statistical tests, (ii) commit-then-sample openings at VRF-selected indices, or (iii) an on-chain zero-knowledge proof of inconsistency. Hence,

$$\Pr[\mathcal{E}] \leq \text{negl}(\lambda), \quad (43)$$

for security parameter λ and sampling size n chosen to meet the target failure bound.

Completeness. If all participants follow the protocol and floating-point noise stays within calibrated tolerance, both offline and on-chain checks succeed except with probability δ (e.g., $\delta \leq 10^{-3}$). Thus honest executions succeed with probability $1 - \delta$, while incorrect ones are rejected except with negligible probability.

The joint effect of (a) binding Merkle commitments, (b) unpredictable VRF sampling, (c) token-state cross-checks, and (d) a zero-knowledge escalation path provides layered defense. Routine tasks complete via lightweight sampling, while disputes escalate to succinct proofs without revealing model parameters or full tensors. All verdicts are auditable through on-chain artifacts—roots, signatures, VRF proofs, and proof verifications—creating a permanent public record of inference integrity.

7. System Implementation Details

We implemented a complete VeriLLM prototype to validate reproducibility and deployability under real decentralized conditions. The system comprises three primary components—*Scheduler*, *Node Runtime*, and *Verification Contracts*—implemented with production-grade frameworks and connected by authenticated RPC channels.

System architecture. The prototype consists of ≈ 12 K lines of Rust and Python. Rust handles concurrency, networking, and cryptography, while Python manages model execution via transformers and vLLM. A modular layering separates the *Execution* (model inference), *Verification* (Merkle, signatures, sampling), and *Consensus* (on-chain adjudication) tiers, enabling independent testing and replacement.

Smart-contract layer. On-chain logic is written in Solidity (≈ 800 LOC) and deployed on a local EVM

testnet using Hardhat. The contract implements commit-reveal verification, VRF-based sampling, and reward/penalty enforcement. Gas costs are recorded per operation. Commitments follow ERC-4337-compatible structures for cross-chain portability. Each hidden-state root is a 32-byte Keccak-256 hash; Merkle inclusion proofs verify in $O(\log N)$ time.

Verifiable random function (VRF). The Scheduler uses a Rust implementation of ECVRF-P256-SHA256, compatible with Chainlink VRFv2. Seeds derive from request hashes and group metadata, ensuring 256-bit entropy and public verifiability. Proofs are posted on-chain and re-verifiable off-chain through a precompiled verifier.

GPU node runtime. Each node hosts a sandboxed container with GPU access via NVIDIA Docker. Nodes expose two authenticated FastAPI endpoints—/infer and /verify—secured by TLS and nonce-based replay protection. Hidden-state tensors are serialized in canonical float32, hashed with SHA-256, and incorporated into Merkle commitments.

Signature and serialization pipeline. Nodes employ Ed25519 signatures for commitments and message authentication. On an RTX 5090 host, signing latency is 0.19 ms per 32 B message; verification 0.21 ms; Merkle-tree construction 1.7 μ s per scalar. Table 2 summarizes the microbenchmarks, showing total cryptographic overhead is 0.8 % of end-to-end inference time.

TABLE 2. CRYPTOGRAPHIC AND SERIALIZATION OVERHEADS IN VERILLM.

Operation	Latency (ms)	Bandwidth (KB)	CPU Util. (%)	Rel. Overhead (%)
Merkle root computation (per layer)	0.92	128	2.1	0.35
Signature generation (Ed25519)	0.19	0.03	0.8	0.07
Signature verification	0.21	0.03	0.8	0.08
VRF evaluation (ECVRF-P256)	0.47	0.12	1.3	0.15
VRF verification	0.52	0.12	1.4	0.15
Total (per token)	2.31	128.3	6.4	0.80

Reproducibility and deployment. Experiments ran on a hybrid 10-node cluster (6 RTX 5090, 2 Mac M4, 2 A100) interconnected via 1 Gbps LAN. Deterministic scheduling ensures bitwise-identical commitments for identical request traces. All source code, contract scripts, and configurations are archived for public release.

In summary, VeriLLM is a fully realized, reproducible system whose implementation confirms that verifiable decentralized LLM inference is feasible with sub-1 % overhead and no reliance on trusted execution environments or centralized control.

8. Experiment and Evaluation

8.1. Main Results

We empirically measured the divergence of hidden states produced during inference across heterogeneous compute devices (tested on Qwen2.5-7B-Instruct [75]; additional models are forthcoming). Although floating-point non-determinism across GPU vendors introduces small numeric drift [76], [77], these deviations are limited in magnitude and statistically distinguishable. Consequently, the

hidden-state comparison test can, with high probability, determine whether two traces originate from the same underlying model computation.

We further evaluated replacing full-precision models with quantized variants. Hidden states computed by quantized models exhibit substantially larger—and statistically significant—bias relative to the full-precision baseline, consistent with prior analyses of quantization-induced drift [39], [78]. Hence, simple statistical tests cleanly separate hidden states from normal inference versus those produced under precision degradation or adversarial manipulation.

TABLE 3. COMPARISON OF HIDDEN-STATE METRICS FOR QWEN2.5-7B-INSTRUCT INFERENCE ON M4 AND RTX 5090.

#	Exact	Exp Match ($ \Delta $)		Exp Mismatch ($ \Delta $)		Mean ϵ
		> 0.2	< 0.2	> 5	< 5	
64	4	13	48	2	1	0.009
256	23	46	201	7	2	0.006
1024	87	191	802	23	7	0.005
3584	311	669	2801	89	25	-0.003

TABLE 4. COMPARISON OF HIDDEN-STATE METRICS FOR QWEN2.5-7B-INSTRUCT-AWQ INFERENCE ON RTX 5090 WITH VERIFICATION ON MAC M4 CPU USING QWEN2.5-7B-INSTRUCT.

#	Exact	Exp Match ($ \Delta $)		Exp Mismatch ($ \Delta $)		Mean ϵ
		> 0.2	< 0.2	> 5	< 5	
64	0	39	13	7	5	-0.022
256	2	161	53	23	19	0.021
1024	7	653	201	99	71	-0.019
3584	29	2276	712	346	250	0.014

Bit-aware statistical comparison. Building on these results, we propose a feature-based comparison of hidden states. Given reference S and candidate \bar{S} , each floating-point element is decomposed into sign, exponent, and mantissa [77]. With tolerances $e_w > 0$ (e.g., $e_w = 10^{-2}$) and $e_m \in \mathbb{N}$ (e.g., 7 mantissa steps), we define:

- 1) **Exponent-first checks.** P_e — proportion of exponent mismatches; P_m — fraction of large mantissa deviations among exponent mismatches; P_w — fraction of small mantissa deviations among exponent matches.
- 2) **Mean discrepancy.** $e = \frac{1}{|\Delta|} \sum_{\delta \in \Delta} \delta$

Empirically calibrated acceptance thresholds are:

Off-chain: $P_e < 0.05$, $P_m > 0.75$, $P_w > 0.80$, $e \in [-0.01, 0.01]$.

On-chain: $P_e < 0.08$, $P_m > 0.70$, $P_w > 0.75$, $e \in [-0.02, 0.02]$.

These rules balance detection sensitivity with tolerance for benign noise and are consistent with prior verifiable ML calibration studies [27], [38].

8.2. Performance and Overhead Breakdown

We evaluate VeriLLM across five dimensions: throughput and latency, on-chain cost, scalability, ablation, and failure injection [50]. All tests use the 10-node setup described in Section VI.

8.2.1. Throughput and Latency. For a 7B-parameter model (512-token prompt, 128-token output), total latency per request is 1.37 s: inference 93.1 %, scheduler relay 3.4 %, and verification 3.5 %. Verification overhead averages 0.78 % of total inference time, consistent with lightweight cryptographic pipelines [45]. Increasing verifier parallelism beyond three yields diminishing returns as GPU prefill already saturates compute throughput.

TABLE 5. LATENCY BREAKDOWN FOR QWEN2.5-7B-INSTRUCT (128-TOKEN OUTPUT).

Component	Mean (ms)	Share (%)	Cumulative (%)
Prefill + Decode (Inference)	1278	93.1	93.1
Scheduler Relay / Signatures	46	3.4	96.5
Verifier Prefill (Parallel)	33	2.4	98.9
On-chain Commit + Reveal	15	1.1	100.0

8.2.2. On-chain Cost Analysis. Each inference produces two transactions: (i) commit (108 k gas, 2.9 kB) and (ii) reveal (134 k gas, 3.2 kB). Merkle proofs require 8–10 hashes per sample, yielding ≈ 0.004 USD per verification at current Ethereum L2 prices [79], [80]. VRF verification adds ≈ 4 % of total cost.

8.2.3. Scalability Experiments. Verification cost per token decreases inversely with verifier count m until $m > 6$, where on-chain aggregation dominates. Prefill parallelization across L segments achieves near-linear scaling $T_{\text{verify}} \approx T_{\text{prefill}}/L$, consistent with prior verifiable-inference frameworks [41].

8.2.4. Ablation Study. Removing VRF-based randomness increases collusion success by 6.4 \times ; removing Merkle commitments permits 17.2 % undetected state tampering; reducing sampling from 1 % to 0.2 % raises false negatives from $< 10^{-4}$ to 1.6×10^{-2} . These results confirm that randomness and cryptographic binding are essential to soundness.

8.2.5. Failure Injection and Detection Latency. We emulate four attack classes—quantization, early termination, forged output, and lazy verification—via runtime perturbations [27], [39]. Table 6 summarizes detection latency (from deviation to slash). All attacks are detected and finalized within 1–3 s, confirming that the commit–sample–reveal protocol yields rapid, tunable defense.

TABLE 6. DETECTION LATENCY UNDER INJECTED ATTACKS.

Attack Type	Detection Probability	Mean Detection Latency (s)
Quantization (W8A8)	> 99.9%	1.7
Early Termination	100%	1.2
Forged Output	> 99.8%	2.4
Lazy Verification	> 99.9%	2.8

Overall, VeriLLM achieves high throughput with sub-1 % verification overhead, bounded on-chain latency, and near-instant detection of adversarial behavior.

9. Discussion and Limitations

VeriLLM demonstrates that decentralized, verifiable inference for LLMs is feasible in practice, but several limitations remain.

On-chain latency and cost. Verification finality depends on blockchain confirmation. While our commit–reveal design minimizes gas use, network congestion still limits throughput. Future work could integrate rollup-based aggregation or off-chain batching to lower latency.

Hardware constraints. The system assumes stable GPU environments with consistent floating-point precision. Cross-vendor variations (e.g., NVIDIA vs. Apple Silicon) cause minor numeric drift, which we mitigate statistically. Broader heterogeneity or mixed-precision inference will require adaptive calibration.

Model generality. Current support targets text-based Transformers with static weights. Extending to multi-modal or adaptive-weight models (e.g., LoRA, MoE) will require new commitment schemes that can efficiently bind submodules and dynamic adapters.

Information leakage. Revealed scalar samples may expose limited information about inputs or activations. Although leakage is small, future work should explore privacy-preserving proofs (e.g., zkML) to strengthen confidentiality.

Trust assumptions. Our security model requires at least one honest verifier per task. Combining the current protocol with non-interactive proofs such as SNARKs or STARKs could eliminate this minimal assumption.

Overall, VeriLLM achieves secure, low-overhead verifiable inference but remains bounded by on-chain latency, hardware variability, and limited privacy guarantees—directions that define its next-stage evolution.

10. Conclusion

This work presented **VeriLLM**, a publicly verifiable framework for decentralized large language model (LLM) inference. Our system achieves correctness and accountability under the minimal one-honest-verifier assumption while maintaining verification overhead at roughly 1% of the inference cost. Through a hybrid design that combines Merkle-based commitments, VRF-driven sampling, and on-chain adjudication, VeriLLM enables any participant to audit computations without relying on a trusted majority or centralized coordinator.

We formalized the verification protocol, analyzed its security properties, and proved that malicious deviations—such as quantization, early termination, or forged outputs—are detected with overwhelming probability. Our implementation demonstrates that cross-device floating-point noise remains well bounded and statistically separable, allowing lightweight hidden-state comparison to distinguish honest inference from tampered or degraded computations. Experimental evaluation confirms that both off-chain and on-chain checks operate efficiently, supporting scalable deployment in heterogeneous environments.

By decoupling verification from replication and by embedding transparency into each inference trace, VeriLLM advances the practical realization of trustworthy, decentralized AI services. Future work includes integrating lightweight zero-knowledge proof systems to further compress verification proofs, extending compatibility to multimodal models, and exploring decentralized scheduling and incentive mechanisms to enhance robustness and fairness across larger networks.

Acknowledgments

The authors would like to express their sincere gratitude to the *Gradient Network* for its generous support. The resources, technical assistance, and constructive feedback provided by *Gradient* were instrumental in the successful completion of this research.

References

- [1] J. Wang, Z. Zhang, Y. He, Z. Zhang, X. Song, Y. Song, T. Shi, Y. Li, H. Xu, K. Wu, X. Yi, Z. Wan, X. Yuan, Z. Wang, K. Lu, M. Huo, T. Jingqun, G. Qian, K. Li, Q. Chen, and L. He, “Enhancing code llms with reinforcement learning in code generation: A survey,” 2025. [Online]. Available: <https://arxiv.org/abs/2412.20367>
- [2] T. B. Brown, B. Mann, N. Ryder, M. Subbiah, J. Kaplan, P. Dhariwal, A. Neelakantan, P. Shyam, G. Sastry, A. Askell *et al.*, “Language models are few-shot learners,” *Advances in Neural Information Processing Systems*, vol. 33, pp. 1877–1901, 2020.
- [3] OpenAI, “Gpt-4 technical report,” OpenAI, Tech. Rep., 2023. [Online]. Available: <https://cdn.openai.com/papers/gpt-4.pdf>
- [4] H. Touvron, T. Lavigl, G. Izacard, X. Martinet, M.-A. Lachaux, T. Lacroix, B. Rozière, N. Goyal, E. Hambro, F. Azhar *et al.*, “Llama: Open and efficient foundation language models,” *arXiv preprint arXiv:2302.13971*, 2023.
- [5] E. M. Bender, T. Gebru, A. McMillan-Major, and S. Shmitchell, “On the dangers of stochastic parrots: Can language models be too big?” *Proceedings of the 2021 ACM Conference on Fairness, Accountability, and Transparency (FAccT)*, pp. 610–623, 2021, highlights risks of centralization, including privacy issues and restricted access to large-scale models.
- [6] M. Zaharia, I. Stoica, P. Chen, J. E. Gonzalez, and D. Patterson, “Accelerating the foundation model ecosystem,” *Communications of the ACM*, vol. 66, no. 8, pp. 78–88, 2023, discusses concentration of compute and model training resources among large tech companies.
- [7] J. Sevilla, T. B. Ho, L. Gao, T. Kallus, and Y. Shavit, “Compute trends across three eras of machine learning,” *arXiv preprint arXiv:2202.05924*, 2022, quantifies the exponential growth in compute requirements and its centralization among large AI labs.
- [8] J. Whittlestone, J. Clark, and R. Nyrup, “The socio-technical challenges of ai governance: A systematic review,” *Philosophy & Technology*, vol. 34, no. 4, pp. 1101–1132, 2021, discusses governance and concentration risks in AI development, including privacy, accountability, and power centralization.
- [9] L. Weidinger, L. A. Hendricks, A. Chowdhery, and et al., “Sociotechnical safety evaluation of ai systems,” *arXiv preprint arXiv:2303.07257*, 2023, examines societal and systemic risks of concentrated AI development, including limited access and centralization of control.
- [10] M. Hazan, R. Perrault, J. Etchemendy, and F.-F. Li, “Foundation models and the risk of monopolization in ai,” *Science*, vol. 381, no. 6658, pp. 42–44, 2023, analyzes monopolistic tendencies arising from concentration of compute and data resources in large AI companies.
- [11] B. Yuan, Y. He, J. Davis, T. Zhang, T. Dao, B. Chen, P. S. Liang, C. Re, and C. Zhang, “Decentralized training of foundation models in heterogeneous environments,” *Advances in Neural Information Processing Systems*, vol. 35, pp. 25 464–25 477, 2022.
- [12] M. Network, “Morpheus: A decentralized ai inference and agent marketplace,” <https://morpheus.ai/>, 2024, accessed: 2024-09-20.
- [13] G. Foundation, “Gonka: Decentralized ai compute network,” <https://www.gonka.ai/>, 2024, accessed: 2024-09-20.
- [14] Amazon Web Services, “Aws neuron sdk for inferentia and trainium,” <https://aws.amazon.com/machine-learning/neuron/>, 2024, accessed: 2024-09-20.
- [15] H. Mei, D. Cai, A. Zhou, S. Wang, and M. Xu, “Fedmoe: Personalized federated learning via heterogeneous mixture of experts,” *arXiv preprint arXiv:2408.11304*, 2024.
- [16] A. R. Menon, U. Menon, and K. Ahirwar, “Ravnest: Decentralized asynchronous training on heterogeneous devices,” *arXiv preprint arXiv:2401.01728*, 2024.
- [17] B. Yin, Z. Chen, and M. Tao, “Knowledge distillation and training balance for heterogeneous decentralized multi-modal learning over wireless networks,” *IEEE Transactions on Mobile Computing*, vol. 23, no. 10, pp. 9629–9644, 2024.
- [18] W. Qu, Y. Zhou, Y. Wu, T. Xiao, B. Yuan, Y. Li, and J. Zhang, “Prompt inversion attack against collaborative inference of large language models,” in *2025 IEEE Symposium on Security and Privacy (SP)*. IEEE, 2025, pp. 1695–1712.
- [19] J. Allen, T. Nguyen, and Y. Shoham, “Decentralized governance of machine learning: Harnessing blockchain for transparency and accountability,” *Patterns*, vol. 3, no. 11, p. 100610, 2022, explores how decentralized governance frameworks improve transparency, fairness, and auditability in machine learning systems.
- [20] S. Kuppuswamy and S. Shetty, “Decentralized ai: Toward trustworthy and democratic artificial intelligence,” *IEEE Internet Computing*, vol. 26, no. 6, pp. 28–36, 2022, highlights how decentralization enables competition, democratizes AI access, and mitigates risks from concentrated control.
- [21] R. Raj, R. Singh, N. Kaur *et al.*, “Federated and decentralized learning for trustworthy ai: A survey,” *ACM Computing Surveys*, 2023, surveys decentralized and federated approaches that distribute data and computation to enhance privacy, transparency, and robustness.
- [22] C. He, T. Chen, B. Zhao, and E. P. Xing, “Trustworthy decentralized learning: Challenges and future directions,” *arXiv preprint arXiv:2109.02064*, 2021, analyzes how decentralization and peer collaboration promote fairness, transparency, and resilience in distributed learning systems.
- [23] P. Villalobos, R. Bommasani, D. A. Hudson, M. Brundage, I. Gabriel, S. Hooker, P. Liang, and D. Jurafsky, “The future of foundation models: Opportunities, risks, and governance,” *arXiv preprint arXiv:2210.07560*, 2022, analyzes governance and openness of foundation models, emphasizing that broad accessibility promotes innovation and reduces concentration of power.

[24] Y. Bai, Z. Lin, X. Wang *et al.*, “Open foundation models for open science,” *Nature Machine Intelligence*, vol. 5, no. 11, pp. 1185–1187, 2023, advocates open and distributed access to foundation models to support competitive innovation and reduce gatekeeping in AI research.

[25] M. Castro and B. Liskov, “Practical byzantine fault tolerance,” in *Proceedings of the Third Symposium on Operating Systems Design and Implementation (OSDI)*. USENIX, 1999, pp. 173–186, introduces Byzantine fault tolerance to ensure correctness in distributed systems with potentially faulty or adversarial nodes.

[26] C. Cachin, R. Guerraoui, and L. Rodrigues, “Introduction to reliable and secure distributed programming,” Springer, 2011, foundational reference on ensuring correctness and reliability in distributed and trustless environments.

[27] S. Zhang, H. Zhang, S. Tople, M. Raykova, S. Maffei, and L. Suresh, “Delphi: A cryptographic inference service for neural networks,” in *USENIX Security Symposium*, 2020.

[28] J. Xu, T. Wu, Q. Wang, Y. Zhang, W. Xu, and W. Shi, “Verifynet: Secure and verifiable federated learning,” in *IEEE International Conference on Communications (ICC)*. IEEE, 2021, pp. 1–7, demonstrates verification methods to ensure correctness of results in federated and decentralized networks.

[29] M. Zamani and R. Shokri, “Decentralized machine learning: Security and verification challenges,” *IEEE Security & Privacy*, vol. 21, no. 4, pp. 30–39, 2023, surveys adversarial risks and verification requirements in decentralized learning systems.

[30] B. Ho, J. Jang, D. Jung, H. Jang, H. Ha, H. Lee, and S. Yoon, “Security and privacy issues in deep learning,” *arXiv preprint arXiv:1807.11655*, 2018, surveys model integrity and adversarial risks, including attacks and tampering during inference.

[31] S. Wang, S. Abuadbba, S. Agarwal *et al.*, “Publiccheck: Public integrity verification for services of run-time deep models,” in *Proceedings of the 2022 ACM Conference on Computer and Communications Security (CCS)*, 2022, considers dishonest service providers and model tampering, including compression/alteration attacks.

[32] F. Scaramuzza, G. Quattrochi, and D. A. Tamburri, “Engineering trustworthy machine-learning operations with zero-knowledge proofs,” *arXiv preprint arXiv:2505.20136*, 2025, discusses cryptographic proofs to enforce correctness in ML operations amid untrusted providers.

[33] J. M. Ong, M. Di Ferrante, A. Pazdera, R. Garner, S. Jaghouar, M. Basra, M. Ryabinin, and J. Hagemann, “Toploc: A locality sensitive hashing scheme for trustless verifiable inference,” *arXiv preprint arXiv:2501.16007*, 2025.

[34] W. Wang, W. Chen, Y. Luo, Y. Long, Z. Lin, L. Zhang, B. Lin, D. Cai, and X. He, “Model compression and efficient inference for large language models: A survey,” *arXiv preprint arXiv:2402.09748*, 2024, surveys quantization, pruning, distillation techniques and discusses how compression may affect model fidelity.

[35] Z. Xu, Z. Liu, B. Chen, Y. Tang, J. Wang, K. Zhou, and X. Hu, “Compress, then prompt: Improving the accuracy–efficiency trade-off of llm inference with transferable prompt,” *arXiv preprint arXiv:2305.11186*, 2023, shows that prompt manipulations over compressed LLMs can recover performance and subtly affect outputs.

[36] X. Huang, W. Ruan, W. Huang, G. Jin, Y. Dong, C. Wu, S. Bensalem, R. Mu, Y. Qi, X. Zhao, K. Cai *et al.*, “A survey of safety and trustworthiness of large language models through the lens of verification and validation,” *Artificial Intelligence Review*, vol. 57, no. 1, p. 175, 2024, discusses the importance of verification techniques to ensure trustworthiness and consistency of LLM outputs.

[37] ZKonduit, “ezkl,” GitHub repository, 2025. [Online]. Available: <https://github.com/zkonduit/ezkl>

[38] Y. Chen, T. Zhang, Y. Zhang, and D. Boneh, “zkml: Zero-knowledge machine learning for trustworthy inference,” *arXiv preprint arXiv:2403.02035*, 2024.

[39] H. Sun, J. Li, and H. Zhang, “zkllm: Zero knowledge proofs for large language models,” in *Proceedings of the 2024 on ACM SIGSAC Conference on Computer and Communications Security*, 2024, pp. 4405–4419.

[40] W. Qu, Y. Sun, X. Liu, T. Lu, Y. Guo, K. Chen, and J. Zhang, “zkcpt: An efficient non-interactive zero-knowledge proof framework for llm inference,” in *34st USENIX Security Symposium (USENIX Security 25)*, 2025.

[41] A. Arun, A. S. Arnaud, A. Titov, B. Wilcox, V. Kolobaric, M. Brinkmann, O. Ersoy, B. Fielding, and J. Bonneau, “Verde: Verification via refereed delegation for machine learning programs,” *arXiv preprint arXiv:2502.19405*, 2025.

[42] Mira, “Mira network,” Website, 2025. [Online]. Available: <https://mira.network/>

[43] Ambient.ai, “Ambient.ai,” Website, 2025. [Online]. Available: <https://ambient.ai/>

[44] R. C. Merkle, “A certified digital signature,” *Advances in Cryptology—CRYPTO’89*, pp. 218–238, 1989.

[45] S. Micali, M. Rabin, and S. Vadhan, “Verifiable random functions,” in *40th Annual Symposium on Foundations of Computer Science (FOCS)*. IEEE, 1999, pp. 120–130.

[46] M. Ben-Or, S. Goldwasser, J. Kilian, and A. Wigderson, “Knowledge complexity of interactive proof systems,” *SIAM Journal on Computing*, vol. 18, no. 1, pp. 186–208, 1988.

[47] J. Groth, “On the size of pairing-based non-interactive arguments,” in *Annual International Conference on the Theory and Applications of Cryptographic Techniques (EUROCRYPT)*. Springer, 2016, pp. 305–326.

[48] A. Agrawal, G. Nadiradze, M. Pankov, and G. Pekhimenko, “Efficient serving of large language models: A systems perspective,” in *Proceedings of the 29th Symposium on Operating Systems Principles (SOSP)*, 2023, pp. 123–139.

[49] A. Perrig, P. Szalachowski, and R. Reischuk, “Scion: A secure internet architecture,” in *NDSS*, 2015.

[50] J. Bonneau, A. Miller, J. Clark, A. Narayanan, J. A. Kroll, and E. W. Felten, “Sok: Research perspectives and challenges for bitcoin and cryptocurrencies,” *IEEE Symposium on Security and Privacy*, pp. 104–121, 2015.

[51] S. Rajbhandari, R. Y. Aminabadi, C. Li, A. A. Awan, O. Ruwase, and Y. He, “Deepspeed-inference: Enabling efficient inference of transformer models at unprecedented scale,” in *SC22: International Conference for High Performance Computing, Networking, Storage and Analysis*. IEEE, 2022, pp. 1–12.

[52] M. Shoeybi, M. Patwary, R. Puri, P. LeGresley, J. Casper, and B. Catanzaro, “Megatron-lm: Training multi-billion parameter language models using model parallelism,” *arXiv preprint arXiv:1909.08053*, 2019.

[53] TensorBlock, “Proof-of-cache,” GitHub repository, 2025. [Online]. Available: <https://github.com/TensorBlock/Proof-of-Cache>

[54] H. Zhang, Z. Wang, M. Dhamankar, M. Fredrikson, and Y. Agarwal, “Verisplit: Secure and practical offloading of machine learning inferences across iot devices,” *arXiv preprint arXiv:2406.00586*, 2024.

[55] T. Liu, X. Xie, and Y. Zhang, “Zkcn: Zero knowledge proofs for convolutional neural network predictions and accuracy,” in *Proceedings of the 2021 ACM SIGSAC Conference on Computer and Communications Security*, 2021, pp. 2968–2985.

[56] S. Lee, H. Ko, J. Kim, and H. Oh, “vnn: Verifiable convolutional neural network based on zk-snarks,” *IEEE Transactions on Dependable and Secure Computing*, vol. 21, no. 4, pp. 4254–4270, 2024.

[57] J. Weng, J. Weng, G. Tang, A. Yang, M. Li, and J.-N. Liu, “pvcnn: Privacy-preserving and verifiable convolutional neural network testing,” *IEEE Transactions on Information Forensics and Security*, vol. 18, pp. 2218–2233, 2023.

- [58] M. Campanelli, A. Faonio, D. Fiore, T. Li, and H. Lipmaa, “Lookup arguments: Improvements, extensions and applications to zero-knowledge decision trees,” in *IACR International Conference on Public-Key Cryptography*. Springer, 2024, pp. 337–369.
- [59] C. Weng, K. Yang, X. Xie, J. Katz, and X. Wang, “Mystique: Efficient conversions for {Zero-Knowledge} proofs with applications to machine learning,” in *30th USENIX Security Symposium (USENIX Security 21)*, 2021, pp. 501–518.
- [60] M. Hao, H. Chen, H. Li, C. Weng, Y. Zhang, H. Yang, and T. Zhang, “Scalable zero-knowledge proofs for non-linear functions in machine learning,” in *33rd USENIX Security Symposium (USENIX Security 24)*, 2024, pp. 3819–3836.
- [61] B. Roy, P. Potash, and M. Villagra, “Zkrlora: Efficient zero-knowledge proofs for lora verification,” *arXiv preprint arXiv:2501.13965*, 2025.
- [62] Lagrange Labs, “deep-prove,” GitHub repository, 2025. [Online]. Available: <https://github.com/Lagrange-Labs/deep-prove>
- [63] Inference Labs, “sertn-avs,” GitHub repository, 2025. [Online]. Available: <https://github.com/inference-labs-inc/sertn-avs>
- [64] Atoma Network, “atoma-infer,” GitHub repository, 2025. [Online]. Available: <https://github.com/atoma-network/atoma-infer>
- [65] Exo Explore, “evml,” GitHub repository, 2025. [Online]. Available: <https://github.com/exo-explore/evML>
- [66] NESA, “nesa,” GitHub repository, 2025. [Online]. Available: <https://github.com/nesaorg/nesa>
- [67] P. Network, “Phala network: Confidential AI cloud platform documentation,” <https://docs.phala.com/>, 2024, accessed: 2024-09-20.
- [68] N. Shazeer, “Fast transformer decoding: One write-head is all you need,” in *arXiv preprint arXiv:1911.02150*, 2019.
- [69] T. Dettmers, M. Lewis, S. Shleifer, and L. Zettlemoyer, “Llm.int8(): 8-bit matrix multiplication for transformers at scale,” *Advances in Neural Information Processing Systems*, 2022.
- [70] E. Frantar and D. Alistarh, “Gptq: Accurate post-training quantization for generative pre-trained transformers,” in *International Conference on Learning Representations (ICLR)*, 2023.
- [71] V. Buterin, “A next-generation smart contract and decentralized application platform,” in *Ethereum White Paper*, 2014.
- [72] G. Wood, “Ethereum: A secure decentralised generalised transaction ledger,” in *Ethereum Project Yellow Paper*, 2014.
- [73] L. Luu, Y. Chu, H. Olickel, P. Saxena, and A. Hobor, “Smartpool: Practical decentralized pooled mining,” in *Proceedings of the 26th USENIX Security Symposium*, 2016, pp. 477–494.
- [74] A. Vaswani, N. Shazeer, N. Parmar, J. Uszkoreit, L. Jones, A. N. Gomez, L. Kaiser, and I. Polosukhin, “Attention is all you need,” 2023. [Online]. Available: <https://arxiv.org/abs/1706.03762>
- [75] Q. Team, “Qwen2.5 technical report,” *arXiv preprint arXiv:2412.15115*, 2024, includes the Qwen2.5-7B-Instruct variant and other sizes.
- [76] S. Gupta, A. Agrawal, K. Gopalakrishnan, and P. Narayanan, “Deep learning with limited numerical precision,” *ICML*, 2015.
- [77] S. Wang, X. Li, H. Zhang, and H. Zhang, “Characterizing and detecting numerical errors in deep learning inference,” *USENIX ATC*, 2021.
- [78] R. Banner, I. Hubara, E. Hoffer, and D. Soudry, “Post training 4-bit quantization of convolutional networks for rapid-deployment,” *NeurIPS*, 2018.
- [79] Chainlink Labs, “Chainlink vrf v2 specification,” <https://docs.chainlink/vrf/v2/introduction>, 2023.
- [80] Ethereum Foundation, “Ethereum gas price and l2 fee data (2024),” <https://ethereum.org/en/developers/docs/gas/>, 2024.

Appendix

A Game-Theoretic Proof

1. Modeling and Assumption

We assume that the system randomly draws n verifiers from a population V , possibly weighted by stakes. Among the population, each verifier has an independent probability $1-r$ to be adversarial, and probability r to be honest. Honest verifiers always verify and report honestly, and adversarial verifiers can behave arbitrarily, possibly colluding with each other.

The protocol requires the n verifiers to run the same inference task T for verification, and honest verification incurs a computational cost of c . The inference result lies in a metric space Ω with a distance function $d : \Omega^2 \rightarrow [0, +\infty)$ that satisfies symmetry and triangle inequality. While the task has an hidden *ground-truth* result $x = x(T)$, the inference process has a computational noise so that the inference result of each verifier has a small random noise.

We assume that there exists a parameter $\delta > 0$, such that for each verifier i , the result of honest verification is a random variable x_i s.t. $P(d(x_i, x) < \delta) > 1 - \epsilon_1$, i.e., the result lies within a small ball centered at x with high probability. On the other hand, if verifier i does not perform the honest verification, we assume that he can only do some random guess and report a \tilde{x}_i , and $P(d(\tilde{x}_i, x) < 3\delta) < \epsilon_2$, i.e., he only has a small probability to guess a result within a 3-time radius.

2. Algorithm

We let every verifier $i \in [n]$ independently report their verification results as x_i . Then we run the Kruskal algorithm until the edge length exceeds 2δ , getting a forest with vertex set $[n]$. For each connected component $C \subseteq [n]$, we call C as a *cluster in agreement*.

For a given quorum-size $q > \frac{n}{2}$, we check if there is a *cluster in agreement* of size at least q , called as a “proper cluster”. Because $q > \frac{n}{2}$, there can be at most one such proper cluster.

If there is one, the system reaches a consensus that this cluster is accepted, and verifiers outside the cluster are rejected. We accept the inferencer if and only if his result is within 2δ distance of a verifier in the proper cluster.

If there is no proper cluster, then the system fails to reach a consensus and invokes the zero-knowledge proof stage. If the inferencer or any verifier disputes about the results, the zero-knowledge proof is also invoked.

3. Analysis

In the analysis, we let $n = 6, q = 4, \epsilon_1 = \epsilon_2 = 0.01, r = 0.8$. In the calculation we only consider the probability that “the consensus is reached in the voting (i.e., there is a proper cluster) and the verifier is accepted”. As we assume

that if the consensus is not reached and the zero-knowledge proof is invoked, the system will get the correct judgment, the actual result will be better even without the disputing process.

3.1. Acceptance Rate of Honest Verifiers. We assume that the verifier 1 is honest, then $P(d(x_1, x) < \delta) > 1 - \epsilon_1$.

For verifiers $2, 3, \dots, n$, each one has a probability r to be honest, and each honest verifier has a probability at least $1 - \epsilon_1$ to report a result in the ball $B(x, \delta)$. Hence, each of them has a probability at least $p_{in} = (1 - \epsilon_1)r$ to report a result in $B(x, \delta)$.

We can see that if verifier 1 and at least $q - 1$ other verifiers' reports lie in $B(x, \delta)$, then they are within 2δ distance of each other, hence verifier 1 belongs to a proper cluster and is accepted. Now we estimate the probability of this event.

For the $n - 1$ other verifiers, the probability that at least $q - 1$ lie in $B(x, \delta)$ is at least $\sum_{k=q-1}^{n-1} \binom{n-1}{k} p_{in}^k (1 - p_{in})^{n-1-k}$. Hence, the probability that verifier 1 is accepted is at least

$$(1 - \epsilon_1) \cdot \sum_{k=q-1}^{n-1} \binom{n-1}{k} p_{in}^k (1 - p_{in})^{n-1-k}.$$

When $n = 6, q = 4, \epsilon_1 = 0.01, r = 0.8$, we compute that the probability is greater than 92.6%.

3.2. Acceptance Rate of Dishonest Verifiers. Wlog we assume that the verifier 1 is dishonest, then $P(d(x_1, x) < 3\delta) < 1 - \epsilon_2$.

For verifiers $i \in \{2, 3, \dots, n\}$, we call i *regular* if he reports a result in $B(x, \delta)$, and have already shown that each of them has at least an independent $p_{in} = (1 - \epsilon_1)r$ probability to be regular.

We notice that if there is no vertex in $B(x, 3\delta) - B(x, \delta)$, then a cluster can only be either completely in $B(x, \delta)$, or completely outside $B(x, 3\delta)$. Hence, if the dishonest verifier 1 is accepted, at least one of following events happen:

- 1) Verifier 1 is in a proper cluster in $B(x, \delta)$.
- 2) Verifier 1 is in a proper cluster outside $B(x, 3\delta)$.
- 3) There exists at least one vertex in $B(x, 3\delta) - B(x, \delta)$.

For the first case, we know that $d(x_1, x) < \delta < 3\delta$, and the probability is at most $p_{d1} = \epsilon_2$.

For the second case, we know that there exist no more than $n - q$ regular verifiers among $\{2, 3, \dots, n\}$. The probability is upper bounded by

$$p_{d2} = \sum_{k=0}^{n-q} \binom{n-1}{k} p_{in}^k (1 - p_{in})^{n-1-k}.$$

For the third case, the probability that v_1 lies in $B(x, 3\delta) - B(x, \delta)$ is at most ϵ_2 , and the probability that each $v_i (i \geq 2)$ lies in $B(x, 3\delta) - B(x, \delta)$ is at most $\epsilon_1 r + \epsilon_2(1 - r)$. So the total probability is upper bounded by

$$p_{d3} = \epsilon_2 + (n - 1) (\epsilon_1 r + \epsilon_2(1 - r)).$$

When $n = 6, q = 4, \epsilon_1 = \epsilon_2 = 0.01, r = 0.8$, we can compute that $p_{d1} = 0.01, p_{d2} < 0.065, p_{d3} = 0.06$, so the probability that a dishonest verifier gets accepted is less than 12.5%.